R. & M. No. 3690

R. & M. No. 3690

MINISTRY OF DEFENCE (PROCUREMENT EXECUTIVE)
AERONAUTICAL RESEARCH COUNCIL
REPORTS AND MEMORANDA

A Study of Dynamic Aeroelastic Effects on the Stability Control and Gust Response of a Slender Delta Aircraft

By E. G. BROADBENT,
Aerodynamics Dept., RAE Farnborough

J. K. ZBROZEK
late of Aerodynamics Dept., RAE Farnborough

and

E. HUNTLEY
University of Sheffield

LONDON: HER MAJESTY'S STATIONERY OFFICE
1972
PRICE £2·10 NET

A Study of Dynamic Aeroelastic Effects on the Stability Control and Gust Response of a Slender Delta Aircraft

By E. G. BROADBENT,
Aerodynamics Dept., RAE Farnborough

J. K. ZBROZEK
late of Aerodynamics Dept., RAE Farnborough
and
E. HUNTLEY
University of Sheffield

Reports and Memoranda No. 3690*
March, 1971

Summary.

In this report four previously unpublished notes, concerned with aeroelastic effects on a particular slender delta aircraft configuration, are collected together.

Some general flutter calculations show that decreasing stiffness leads to instability in the aircraft short period mode whilst the higher frequency modes remain stable. The reasons for the instability and the implications regarding aircraft controllability are examined by means of a much simpler mathematical model. It is shown that the instability is directly attributable to the aerodynamic moments arising from aeroelastic distortion defined by the fundamental chordwise bending mode.

The same mathematical model is used in a study of the bending response of the aircraft to discrete step and ramp gusts. It is found that the dynamic overshoot factor due to chordwise bending can vary within much wider limits than the dynamic overshoot factor due to spanwise bending of a conventional aircraft.

* Replaces A.R.C. 32 779.

LIST OF CONTENTS

PREFACE

During the three–four years around 1960 a great deal of thought was being given in the Royal Aircraft Establishment to the aeroelastic problems of slender wings. Some work done by E. G. Broadbent in 1958, when investigating flutter behaviour of such configurations, led him to the conclusion that although flutter modes appeared to be stable, decreasing structural stiffness led to instability of what is primarily the short period rigid body mode. This instability was attributed to the longitudinal bending modes, spanwise bending being relatively unimportant.

The instability of the short period mode was regarded as being symptomatic of difficult handling and manoeuvre problems and led J. K. Zbrozek to consider a much simplified mathematical model in an attempt to gain better physical insight. The problem was treated by solving the conventional short period equations, modified for aeroelastic effects. Only longitudinal bending was considered and the aeroelastic effects were calculated by the method of successive approximations. The values obtained for period and damping were found to correlate well with Broadbent's results. Zbrozek's main conclusions were that his simple approach was sufficiently accurate for the study of large aeroelastic effects, that aeroelasticity primarily influenced restoring moment and that, whilst the effects upon stability could be easily made small, the effects on controllability could be severe. A further important conclusion was that, from a stiffness point of view, a skin thickness would be required of the order of 50 per cent greater than that needed on the basis of pure strength calculations.

Zbrozek went on to assess the effects of longitudinal bending on the controllability of the slender delta aircraft, again simplifying the analysis as far as possible but this time defining the aircraft dynamics by means of one structural mode together with the two rigid body modes, pitching and heaving. These calculations also gave the same variation of short period frequency and damping established by Broadbent. Zbrozek concluded that the model was a reasonable one for studying the dynamic properties of the elastic aircraft and showed that the loss of longitudinal stability could be quite satisfactorily explained by the aerodynamic moments arising from the elastic distortions defined by the fundamental chordwise bending mode.

Once a reasonable model for the study of the dynamics of a slender aircraft had been established, it was decided that further important questions regarding the aircraft response to turbulence needed to be answered. In keeping with the philosophy so far adopted the analysis was to be kept as simple as possible, and so, as a first stage, Huntley considered the bending response of the flexible aircraft to discrete step and ramp gusts, for one aircraft of fixed stiffness and neglecting the pitching degree of freedom*. The conclusions reached were that values of the dynamic overshoot factor due to lengthwise bending of a slender delta aircraft could vary within much wider limits than the dynamic overshoot factor due to spanwise bending of a conventional aircraft. Flying an aircraft at low speed, say $M = 0{\cdot}4$, into a sharp-edged gust produced a value of the dynamic overshoot factor approaching 3. On the other hand at higher speeds, greater than $M = 0{\cdot}9$, and for gust ramp lengths greater than 100 ft the factor appeared to be less than for a conventional aircraft.

Now, the work by Broadbent and Zbrozek summarised above was written up and given a very limited circulation as RAE Tech. Memos and the work by Huntley issued as an RAE Tech. Note. The Loading Actions Sub-Committee of the Aeronautical Research Council thought that it would be regrettable if the work was lost sight of. For it provided a rather unusual and nice example of the way in which, from an initial rather vague question, ideas were gradually formulated and refined leading eventually to a reasonably complete understanding of the mechanisms involved in the problem. Clearly since the time this work was done, much more sophisticated analyses have been done for Concorde involving many more structural modes and more accurate aerodynamic theories. Further, in the event, the aeroelastic properties of Concorde with its relatively conventional body turned out to be more akin to the properties of some existing aircraft than those of the integrated aircraft studied by Broadbent.

---

* Work was done subsequently by Zbrozek and Huntley on the responses of the same slender aircraft to random turbulence (Refs. 1 and 2 of Part IV).

Notwithstanding these provisos it was agreed that the work should be edited to provide a coherent account and published. Had Zbrozek not unfortunately died before the recommendation could be implemented a definitive version could have been prepared with supplementary calculations done to fill in any gaps. As it was, bearing in mind the time that had elapsed, the best that could reasonably be done was for the papers to be presented as they originally appeared with any known errors corrected and repetitious detail deleted. Inconsistencies in the discussions and conclusions have not been cut out since the development of the ideas as insight was gained was one of the interesting aspects of the exercise. It is hoped that, by and large, the flavour of the original notes has been preserved.

This edited version of the work is written in four parts, each one corresponding to a contribution from one of the three authors. Part I by Broadbent gives the results of the initial calculations which sparked off the investigation; Parts II and III contain the work by Zbrozek on the quasi-static and dynamic aeroelasticity assumptions and Part IV contains Huntley's analysis of the bending response to discrete gusts.

Part 1—Some Aeroelastic Calculations on a Slender Delta Aircraft

by
E. G. BROADBENT

1. *Introduction.*

In an attempt to discover the order of aeroelastic effects that might occur on a slender aircraft some general calculations involving rather simple assumptions were carried out. The work was started in June 1957 soon after receipt of a preliminary communication due to R. H. Plascott and J. R. Collingbourne which discussed the use of a slender delta planform for an aircraft designed to cruise at a Mach number of 1·8 or a little more. This was taken to be just below the range of important thermal effects on a light-alloy structure so that a design Mach number of 2 at 40 000 ft seemed a reasonable assumption for aeroelastic calculations. These conditions give a suitable margin of safety over the cruising conditions which would occur at an appreciably greater altitude. The planform chosen was the larger aircraft discussed by Plascott and Collingbourne, which is a complete delta with 79 degree leading edge sweep, a maximum depth of 12 ft, a total length of 226·8 ft and an all up weight of 695 000 lb.

The form of the calculations was to apply Lagrange's equations in vertical translation, pitch and four elastic modes, two of which represented longitudinal bending, and two spanwise bending. In the main results of the work the spanwise bending modes were unimportant, but the longitudinal flexibility led to a forward shift of the centre of pressure, analogous to that on a conventional swept wing aircraft or that due to fuselage flexibility on a conventional aircraft with an aft tailplane. In the particular form of these calculations, for which skin thickness was the principal variable, this adverse shift of centre of pressure led to dynamic instability for all skin thicknesses less than about 1/4 inch at the assumed height and Mach number. In practice it is likely that other effects would occur first, e.g. complete loss of manoeuvre margin, or considerable loss of longitudinal control. The purpose of the present report is to draw attention to these possibilities that arise from longitudinal flexibility rather than to give quantitative results of precise significance. A few comments are given at the end of this report on other aeroelastic effects.

2. *Assumptions.*

2.1. *Structural Assumptions.*

The nose of the delta is taken as origin; x is measured aft and has the value l at the trailing edge ($l = 226{\cdot}8$ ft) and y is measured spanwise. Non-dimensional co-ordinates ξ and η are used and defined as follows:

$$\xi = x/l$$

and

$$\eta = y/l$$

so that the equation of the leading edge is

$$\xi = \eta \tan \Lambda \qquad (\Lambda \text{ is the leading edge sweep})$$

and of the trailing edge is $\xi = 1$. The mass distribution is assumed to have the form

$$\text{mass/unit area} = \mu = \mu_o(\xi - \eta \tan \Lambda)(1 - \xi) \tag{1}$$

where μ_o is a constant, together with a localised mass for the engine. The distribution equation (1) means that the mass distribution across a fore-and-aft section is symmetric, falling to zero at the edges, and with the local CG at the half chord; this leads to an overall CG at 64·6 per cent of the centre-line chord

($\xi = 0{\cdot}646$). The fully loaded condition was taken so that the all up weight is 695 000 lb. Of this total 83 000 lb represents the engine mass and in the early calculations this was located (following Plascott and Collingbourne) at the tip. Later the engines were transferred to the centre-line at the same fore-and-aft position given by a *CG* at $\xi = 0{\cdot}889$; the corresponding values of η are 0·193 and zero.

The stiffness is assumed to derive entirely from the skin, T inches thick in dural, which is equally effective in bending longitudinally and spanwise. The effects of Poisson's ratio, which would provide a coupling between bending in the two planes at right angles, are completely neglected. The skin is assumed to be complete, with no cutouts; its thickness is neglected in comparison with the depth, and its weight is assumed to be included in the mass distribution given above. The maximum depth of the wing, d_{max}, is 12 ft and the depth d at any other point (ξ, η), is given by

$$\frac{d}{d_{max}} = \left(1 - \frac{\eta^2 \tan^2 \Lambda}{\xi^2}\right)(4{\cdot}63039\,\xi^3 - 10{\cdot}63339\,\xi^2 + 6{\cdot}00300\,\xi)\,. \tag{2}$$

This means that the depth on the centre-line rises to a maximum at 37 per cent chord ($\xi = 0{\cdot}37$) and off the centre-line it falls to zero at the leading edge in the form of a parabolic arc along any line of constant ξ. It should be noted that this leads to very small depths near the wing tips, and is much worse for example, than an assumption of constant streamwise sections. The latter assumption would lead to a linear reduction of maximum section thickness from centre-line to tip; but by equation (2) the maximum depth in a streamwise section near the tip derives from the centre-line depths near the trailing edge where they are already small (the second factor in equation (2)) and is then reduced further in moving spanwise (the first factor in equation (2)). It is assumed that there is no external fuselage to bolster up the stiffness near the trailing edge along the centre-line.

The six degrees of freedom allotted to the structure are given by the following equation for the downward displacement, z, of a point (ξ, η) relative to the undisturbed structure in terms of the generalised co-ordinates q_i

$$\frac{z}{l} = q_1 + \xi q_2 + \xi^2 q_3 + \eta^2 q_4 + \xi^3 q_5 + \eta^3 q_6\,. \tag{3}$$

Thus q_1 and q_2 define the amplitudes of the rigid body modes, and for the structural modes (q_3 to q_6) the odd suffixes relate to the modes of longitudinal bending and the even suffixes to the modes of spanwise bending. In the main results q_4 and q_6 are unimportant but we may note that the parabolic and cubic modes chosen do not represent the structure very adequately; the fall off in bending rigidity is so rapid that modes of higher degree in η which would throw more emphasis on the tip region should be considered.

These modes taken individually (other than that of q_1) are unrealistic in that each has a node at the nose of the aircraft, whereas any real mode would have nodes within the area covered by the planform. Provided the modes are used together, however, this does not imply any restriction other than that imposed by the limited number of generalised co-ordinates, since they are free to combine in any linear manner. If, for example, mode 2 were replaced by pitch about the aircraft *CG* so that the second term in equation (3) became $(\xi - \xi_o)\, q_2$ where ξ_o is the value of ξ at the aircraft *CG*, then the only change would be in the calculated values of q_1 and q_2 and not in the physical realism.

2.2. *Aerodynamic Assumptions.*

The basic aerodynamic theory is slender body theory in a rather simple form. The wave equation in terms of the velocity potential ϕ is

$$\frac{\partial^2 \phi}{\partial x^2} + \frac{\partial^2 \phi}{\partial y^2} + \frac{\partial^2 \phi}{\partial z^2} = \frac{1}{a^2}\left(V \frac{\partial}{\partial x} + \frac{\partial}{\partial t}\right)^2 \phi \tag{4}$$

and, as in all forms of slender body theory, the terms in x are neglected. In addition, however, the remaining item on the right hand side of equation (4), i.e. $\frac{1}{a^2}\frac{\partial^2\phi}{\partial t^2}$, is also neglected in order to obtain a simple solution for the generalised forces in the spanwise deformation modes. As regards the main results obtained in this report this second approximation is fully justified because the frequency parameter of the instability is very small. The solution for the generalised forces[1] for the complete wing (tip to tip) can be expressed in the form:

let
$$z = l \sum_i f_i(\xi, \eta)\, q_i \tag{5}$$

and further let
$$f_i(\xi, \eta) = \sum_m g_{im}(\xi) |\eta^m| ; \tag{6}$$

then the generalised force in the i^{th} Lagrangian equation is

$$\sum_j Q_{ij}\, q_j ,$$

where

$$Q_{ij} = \frac{2}{\pi}\rho\, V^2\, l^3\, (\cot \Lambda)^{m+n+2} \sum_m \sum_n \frac{K_m K_n}{m+n+2} \int g_{im}(\xi) \left(\frac{\partial}{\partial \xi} + i\, \nu_0\right) \times$$

$$\times \left\{ \xi^{m+n+2} \left(\frac{\partial}{\partial \xi} + i\, \nu_0\right) g_{jn}(\xi) \right\} d\xi \tag{7}$$

where
$$\nu_0 = \frac{\omega l}{V}$$

and
$$K_m = \frac{\Gamma\left(\frac{m+1}{2}\right)\Gamma(\tfrac{1}{2})}{\Gamma\left(\frac{m}{2}+1\right)}$$

For the modes assumed the only values of K_m needed are K_0, K_2 and K_3 which after substituting for the appropriate gamma functions take the values π, $\frac{1}{2}\pi$ and $4/3$ respectively.

There are one or two points to note about equation (7). The sign of the expression on the right hand side is given as positive, and this is appropriate to the left hand side of the Lagrangian equation so that the coefficients obtained can be used directly in the flutter equations. The expressions as written applies only to a pure delta; for any other planform, as long as the local span increases continuously from nose to trailing edge, replace $(\cot \Lambda)^{m+n+2}$ by $\left(\frac{l}{s}\right)^{m+n}$ where s is the semi-span, and replace ξ^{m+n+2} by η_l^{m+n+2} where η_l is the value of η appropriate to the leading edge and is a known function of ξ. Finally the planform considered here ($\Lambda = 79$ degrees) is not sufficiently slender for the use of slender body theory to

be rigorously justified at a Mach number of 2, but it should not be seriously misleading and it offers the only hope of solutions within a reasonable time*.

2.3. *Solution of the Dynamical Equations.*

The form of Lagrange's equations used is, for the i^{th} equation

$$\frac{d}{dt}\left(\frac{d\overline{T}}{\partial \dot{q}_i}\right)+\frac{\partial \overline{V}}{\partial q_i}+\sum_j Q_{ij}\, q_j = 0 \tag{8}$$

where $\overline{T}$ is the kinetic energy and $\overline{V}$ the strain energy in a generalised displacement.

The expression for $\overline{T}$ is, with μ given by equation (1)

$$\overline{T} = l^4 \int_0^1 d\xi \int_0^{\xi \cot \Lambda} d\eta\, \mu(\xi,\eta)\,(\dot{q}_1+\xi\,\dot{q}_2+\xi^2\,\dot{q}_3+\eta^2\,\dot{q}_4+\xi^3\,\dot{q}_5+\eta^3\,\dot{q}_6)^2+$$

$$+\tfrac{1}{2}\, m_e\, l^2\,(\dot{q}_1+\xi_e\,\dot{q}_2+\xi_e^2\,\dot{q}_3+\eta_e^2\,\dot{q}_4+\xi_e^3\,\dot{q}_5+\eta_e^3\,\dot{q}_6)^2 \tag{9}$$

where m_e is the total engine mass, (ξ_e, η_e) defines the engine CG, and the engine radii of gyration are neglected. The usual factor of 1/2 is absent from the integral in equation (9), because the integral itself is carried out over half the complete aircraft.

The expression for $\overline{V}$ is

$$\overline{V} = \frac{E\,T\,l^2}{2(1-\sigma^2)} \int_0^1 d\xi \int_0^{\xi \cot \Lambda} d\eta\, d^2 \left\{ (\nabla^2 z)^2 - 2(1-\sigma)\left[\frac{\partial^2 z}{\partial x^2}\frac{\partial^2 z}{\partial y^2} - \left(\frac{\partial^2 z}{\partial x\,\partial y}\right)^2\right]\right\}$$

where σ is Poisson's ratio, E is Young's modulus of elasticity and $\nabla^2 \equiv \frac{\partial^2}{\partial x^2}+\frac{\partial^2}{\partial y^2}$. With the assumptions given earlier, including the neglect of σ, this expression becomes

$$\overline{V} = \frac{E\,T\,d_{\max}^2}{2} \int_0^1 d\xi \int_0^{\xi \cot \Lambda} d\eta \left(\frac{d}{d_{\max}}\right)^2 \left\{ \left(\frac{\partial^2 z/l}{\partial \xi^2}\right)^2 + \left(\frac{\partial^2 z/l}{\partial \eta^2}\right)^2 \right\} \tag{10}$$

where $(d/d_{\max})$ is given by equation (2) and (z/l) by equation (3).

For solution it is assumed that the motion is of the form

$$q = \bar{q}\, e^{\lambda \tau} \tag{11}$$

where $\bar{q}$ is independent of time,

$$\tau = \frac{t V_0}{l}.$$

---

*Except possibly for piston theory which would be hard to justify in view of the high leading edge sweep.

and V_0 is a reference speed, here taken to be the true speed appropriate to the design condition of a Mach number of 2 at 40 000 ft.

All the roots of λ are obtained for various values of the skin thickness T inches.

3. *Results and Conclusions.*

In general, for each value of T, there are five conjugate pairs of complex roots for λ; the two remaining roots correspond to unrestrained vertical motion and have no practical importance. Of these roots only one shows any tendency to go unstable and that is the root that represents the short period oscillation of longitudinal dynamic stability, which can be distinguished by its low frequency. For the first set of calculations with the engine at the wing tip the values of this root as the skin thickness is reduced are given in Table 1 up to the point where it goes unstable.

TABLE 1

T (in.)	λ
∞	$-0{\cdot}0734 \pm 0{\cdot}161\,i$
2·0	$-0{\cdot}0705 \pm 0{\cdot}137\,i$
1·0	$-0{\cdot}0650 \pm 0{\cdot}127\,i$
0·5	$-0{\cdot}0584 \pm 0{\cdot}089\,i$
0·375	$-0{\cdot}0526 \pm 0{\cdot}0575\,i$
0·25	$+0{\cdot}0038 \pm 0{\cdot}0219\,i$

It may be noted that the fraction of critical damping (given by the negative ratio of the real part to the imaginary part) increases almost to unity before going unstable. The imaginary part of the roots curresponds with the definition of ν_0 given under equation (7), and to get the frequency in cycles per second it is necessary to multiply by $V_0/2\pi l$ or 1·36. The first sojution, for infinite T, is obtained from the rigid aircraft binary calculation a nd gives a frequency of 0·23 *Hz*.

In case the results were seriously influenced by the engine mass being carried on a very flexible tip the calculation was repeated with the engines transferred to the centre-line. The result was very similar and in this case all five roots are given for two values of T in Table 2.

TABLE 2

T (in.)	λ
0·375	$-0{\cdot}0267 \pm 0{\cdot}0295\,i$
	$-0{\cdot}096 \pm 0{\cdot}91\,i$
	$-0{\cdot}140 \pm 2{\cdot}23\,i$
	$-0{\cdot}072 \pm 10{\cdot}5\,i$
	$-0{\cdot}064 \pm 29\,i$
0·25	$+0{\cdot}0019 \pm 0{\cdot}0105\,i$
	$-0{\cdot}090 \pm 0{\cdot}78\,i$
	$-0{\cdot}149 \pm 1{\cdot}84\,i$
	$-0{\cdot}072 \pm 8{\cdot}6\,i$
	$-0{\cdot}064 \pm 23{\cdot}5\,i$

The instability is seen to be of the same order as before. It is also noteworthy that although the other roots show no sign of instability the damping of the higher frequency modes, i.e. the spanwise bending modes, is very poor.

Finally the mode is given for the short period oscillation in Table 3 for the two values of T.

TABLE 3

$T = 0{\cdot}375$ in.	q_1	$-5{\cdot}25+6{\cdot}73\,i$
	q_2	$+0{\cdot}131+0{\cdot}215\,i$
	q_3	$-0{\cdot}0031-0{\cdot}00045\,i$
	q_4	of order 10^{-5}
	q_5	$+0{\cdot}0041-0{\cdot}00771\,i$
	q_6	of order 10^{-5}
$T = 0{\cdot}25$ in	q_1	$+6{\cdot}18-0{\cdot}219\,i$
	q_2	$+0{\cdot}447+0{\cdot}884\,i$
	q_3	$-0{\cdot}0073+0{\cdot}151\,i$
	q_4	of order 10^{-4}
	q_5	$+0{\cdot}0015-0{\cdot}156\,i$
	q_6	of order 10^{-4}

It can be seen that the amplitudes of the generalised co-ordinates that define longitudinal flexure (q_3 and q_5) show a very rapid increase as the skin thickness is reduced from 0·375 in. to 0·25 in., and are clearly responsible for the instability.

It is apparent from these results that this particular problem deserves more attention. Favourable features are greater depth towards the trailing edge, and any longitudinal stiffening, such as might be possible with a central fin. In addition manoeuvring stability and loss of control should be considered since the effect found here is essentially static in character.

After the basic results, reported above, had been obtained, various modifications to the calculations were tried out to test the importance of some of the assumptions, but the principal result remained substantially unchanged. The modifications included the introduction of structural deformations of higher degree than those represented by equation (3) and also of coupled modes of flexure and torsion, e.g. $\eta^2 \xi^2$, mainly to see if any higher frequency instabilities could be found, but in fact all the high frequency modes remained stable. The effect of a change in planform to an ogee wing with streamwise tips was investigated and also the effect of replacing aerodynamic forces based on slender-body theory with those based on piston theory, but although the magnitude of the results was affected (piston theory gave a smaller range of instability) the general nature of the results was not. The argument for trying the effect of piston theory, despite the highly swept leading edge, was that as the number of nodes along a streamwise section increases, the pressure distribution will come to depend more and more on the local disturbance, as is in fact assumed in piston theory. In all the results obtained, however, it was the fundamental mode of longitudinal flexure that was important, as illustrated by the results of the present paper, and for this mode one would expect slender-body theory to be the more realistic. Moreover slender-body theory also applies at lower Mach numbers where aeroelastic effects could be equally important.

REFERENCE PART I

No.	*Author*	*Title, etc.*
1	D. L. Woodcock	Slender body theory. Chapter 7 of Vol. 2 of the *Manual on Aeroelasticity*. AGARD. 1962.

Part II—Quasi-static Calculations of Dynamic Stability

by
J. K. ZBROZEK

1. *Introduction.*

From the work described by Broadbent it was clear that, whilst the flutter problem appeared not to be a serious one, the dynamic stability and hence aircraft controllability and handling could have been unacceptably bad. The following table summarises those results appertaining to the short period mode as a function of skin thickness T representing aircraft stiffness.

TABLE 1

Skin thickness T, in inches	∞	2 in.	1 in.	0·5 in.	0·375 in.	0·25 in.
Period of oscillations, sec	4·55	5·38	5·31	8·29	12·75	33·6
Damping ratio of oscillations	0·415	0·459	0·455	0·545	0·68	−0·172
Skin to all-up weight ratio		0·96	0·48	0·24	0·18	0·12

The last row in Table 1 shows the ratio of weight of skin alone to total weight. This is meant as an illustration only and the structure weight was assumed to be due to skin thickness only, thus, not-so-small items such as undercarriage, engines, internal structure, etc., were left out. It was assumed that a skin thickness greater than say 0·375 in. would be out of the question. Table 1 shows that the effect of decreasing the structural stiffness by decreasing T is to increase the period of short period oscillations. The damping ratio though not damping itself, at first increases but after reducing skin thickness below some critical value the oscillation becomes divergent. It could be deduced that for T less than say 0·5 in. the handling characteristics of the aircraft would be unacceptable and if a conventional elevator control were used, the skin thickness required would be probably nearer 1 in.

At the time when these results first became available, there was a lack of physical understanding of the whole phenomenon, except that it was thought that the effects were static rather than dynamic in origin. This report describes the attempt made to understand the problem in simple, physical terms and to establish whether the problem was basically connected with the narrow delta configuration, or was due to some other reasons which could possibly be cured by engineering dexterity.

2. *Assumptions.*

The aircraft geometry, its speed and altitude of flight were those given in Part I in order to be able to check the numerical results.

Aerodynamic loading was calculated using piston theory. In simple terms, 'piston theory' means that the air load on a surface element is a function of the incidence of this element only. The incidence could be either due to heaving or due to camber or due to pitching velocity. Piston theory was used as

this theory is amenable to 'back of the envelope' calculations, and it was thought to be good enough for the problem under consideration this being structural rather than aerodynamic in nature. The lift curve slope, using piston theory, was taken to be $\alpha = 4/M = 2$.

The problem was tackled by solving the conventional short period oscillation equations of motion modified for aeroelastic effects.

It was thought originally that aerodynamic and inertia loadings could be lumped together, thus simplifying the calculations, but more careful scrutiny of the equations of motion showed that this was not permissible and aerodynamic and inertia loads had to be treated separately. Thus the aerodynamic moments and forces were calculated without taking account of inertia loading and new moments and forces due to inertia loading were introduced.

All aerodynamic and aeroelastic calculations were made with respect to the *CG* which was found to be at $0{\cdot}635l$ giving a restoring margin of $0{\cdot}032l$. The corresponding values quoted in Part I were $0{\cdot}646l$ and $0{\cdot}021l$ respectively and the discrepancy was attributed to the different methods of accounting for air inertia. The difference was thought to be of no practical significance in the initial stages of the investigation and the restoring margin of $0{\cdot}032l$ was retained for these calculations.

The aircraft was treated as a longitudinal beam with mass and stiffness varying along its length. The aircraft mass distribution used by Broadbent was given by:

$$\text{mass/unit area} = \mu_0 (\xi - \eta \tan \Lambda)(1 - \xi)$$

with ξ, η non-dimensional co-ordinates equal to x/l and y/l respectively, and μ_0 a constant. This expression when integrated with respect to η gave the following longitudinal mass distribution:

$$m(\xi) = 10{\cdot}57 \frac{W}{g} (\xi^2 - \xi^3)$$

where W is the total aircraft weight including the engines (Fig. 1). In addition the engines were represented as a point mass of $0{\cdot}1195\ W/g$ at $\xi = 0{\cdot}889$.

The shape of the wing surface was represented by:

$$\frac{d}{d_{\max}} = \left(1 - \frac{\eta^2 \tan^2 \Lambda}{\xi^2}\right)(4{\cdot}630\ \xi^3 - 10{\cdot}633\ \xi^2 + 6{\cdot}003\ \xi)$$

where $d_{\max}$, the maximum depth, was taken to be 12 feet at $\xi = 0{\cdot}37$. The longitudinal stiffness distribution was then given by:

$$EI = \frac{8}{15} \frac{S}{l} d_{\max}^2\, ET\, \xi\, (4{\cdot}630\ \xi^3 - 10{\cdot}633\ \xi^2 + 6{\cdot}003\ \xi)^2 .$$

This is shown in Fig. 2.

The aeroelastic effects were calculated by the method of successive approximations. It should be mentioned that for skin thickness $T = 0{\cdot}25$ in., the values of the derivatives were rather less reliable than for other thicknesses, due to slow convergence of successive approximations.

3. *Results for Period and Damping Ratio.*

The results of the calculations in terms of period and damping ratio of the short period oscillation are presented in Fig. 3. Fig. 4 shows the amplitude ratio of heaving to pitching velocities, both figures being plotted against the reciprocal of skin thickness. The circles denote the results of Broadbent's calculations.

It can be seen that using the *CG* position of $0{\cdot}635l$ there is no agreement with Broadbent's calculations but upon modifying the calculations to give the *CG* at $0{\cdot}646l$ the agreement for skin thickness greater

than 0·25 in. is amazingly good. This agreement is even more surprising if one remembers that the present calculations were made using a rather simple approach. The conclusion is that for the problem in hand the present approach is probably as good as more sophisticated methods. The only significant difference occurs at a skin thickness of $T = 0{\cdot}25$ in.; the earlier calculations show a divergent oscillation ($\zeta = -0{\cdot}172$) with a period of 33·6 sec, whereas the present study indicates two aperiodic modes, one heavily and the other lightly damped.

4. *Discussion.*

From the remarkable agreement between the present and the earlier calculations (Part 1) it can be concluded that the very simple approach used is sufficient for the study in hand. Both approaches show the same increase in period of oscillation with decreasing skin thickness and the same increase of the damping ratio (Fig. 3). For small skin thickness Broadbent's results indicate oscillatory instability when the present work shows pure divergence. It is interesting to note that the total damping, though not the damping ratio, decreases with decreasing skin stiffness, (Fig. 5) but only very slowly, till some critical value of skin thickness is reached ($T = 0{\cdot}3$ in.) when the oscillation degenerates into two exponential modes. For further decrease of skin thickness, one of the exponential modes becomes less damped, and from extrapolation of calculated results it seems that for $T \doteqdot 0{\cdot}23$ in., this mode becomes divergent. It can be argued that basically there is no disagreement between the two sets of results since both indicate instability only of different forms.

In order to give some idea of the magnitude of the quasi-static aeroelastic effects on calculated moments and forces, some examples are presented in Fig. 6. These are not non-dimensional derivatives but moments and forces in ft lbs and lbs per unit of input. These show that the main effect of flexibility is on the aerodynamic restoring moment M_w (Fig. 6(a)) which is counterbalanced by a moment due to normal acceleration M_n (Fig. 6(b)). The effect of flexibility on other derivatives appears to be comparatively small.

Thus there are two main factors to consider. Firstly, the very delicate balance which exists between aerodynamic and inertia loading distributions and secondly, the great flexibility towards the trailing edge of the aeroplane. Fig. 7 illustrates the relative magnitude of bending moments due to aerodynamic and inertia loading. In this figure the bending moments (in non-dimensional form) due to heaving velocity w are combined with those due to normal acceleration n. It is assumed that normal acceleration is due to heaving velocity only so that both moment distributions are directly comparable. This assumption is very close to the actual state of affairs. The jump in aerodynamic bending moment at the aircraft CG represents the aerodynamic restoring moment and is balanced by appropriate inertia and aerodynamic moments.

It can be seen that the actual bending moment experienced by the structure is the difference between two large quantities and a relatively small redistribution either in aerodynamic or inertia loading could have a very large effect on actual bending. It should be noticed that the resulting bending moment is comparatively large near the trailing edge and remains almost constant long the rest of the rear of the aircraft.

This leads to the second reason for the large aeroelastic effects, namely the assumed stiffness distribution. Fig. 2 shows in non-dimensional form the lengthwise stiffness distribution based on skin thickness of the wing alone. It can be seen that this stiffness decreases very rapidly towards the trailing edge, just where the bending moment is relatively largest. To illustrate this point further Fig. 8 shows a typical lengthwise distribution of wing curvature due to lift loading. It may be noticed that the curvature is largest near the trailing edge, thus being very effective in producing large pitching moments.

The actual shapes of airframe deflection are shown in Figs. 9, 10, and 11, for two skin thicknesses of $T = 1$ in. and $T = 0{\cdot}375$ in. Fig. 9 shows deflection due to the lift alone; this can be visualised as the aircraft being held at its CG at incidence α to the free stream. Fig. 10 shows the deflection due to normal acceleration alone. This again can be portrayed by applying normal acceleration ng at the aircraft CG. The value of acceleration was chosen to satisfy the expression: $nW = aqS\alpha$. This implies that lift and normal acceleration are exactly in phase, which is not very far from the actual facts.

Fig. 11 shows the longitudinal wing deflection due to the combined effects of the lift and corresponding normal acceleration, this deflection being the sum of the deflections shown in Figs. 9 and 10. It can be seen that the wing rhape is such that it produces a large destabilising moment with comparatively small effect on lift; points which are in fact evident from Fig. 6. It can be shown that a relatively small redistribution of stiffness near the trailing edge (behind say $\xi = 0{\cdot}7$ or $0{\cdot}8$) by the addition of fuselage, engine or fin stiffness, can change the magnitude of the problem. A similar argument applies to mass (and aerodynamic load) distribution, except that in this case one has to remember the *CG* and aerodynamic centre will never coincide. Nevertheless, it should be possible to redistribute the bending moments due to inertia.

It might be worth mentioning that from a structural point of view the slender delta is close to the old Junkers idea of a large aircraft in which aerodynamic and inertia loading would be so matched that the structure would have no bending or shear to support. This philosophy provides a new challenge to the designer of slender delta aircraft. There is a large prize in saving structural weight by clever matching of inertia and aerodynamic loads, but also a penalty of danger of instability in numerous aeroelastic modes. Before such a concept would have any practical value, not only would it have to be proved flutter free, but also a new type of control would have to be invented. The controls would need to provide the required moments or forces, not by concentrated forces as given by trailing edge flaps but by evenly and suitably distributed loads. It should be strongly emphasised that the narrow delta is not a stiff aeroplane, it is rather 'a bag of jelly', success of which depends on intelligent matching of stiffnesses and loads.

It is not very clear at this stage how successful the conventional trailing edge controls might be on the narrow delta configuration. There is no doubt that on the configuration studied here trailing edge wide-chord controls would produce formidable difficulties due to their aeroelastic effects. The study of aeroelastic effects on controllability is urgently required, as it may prove that some control shapes tested in wind tunnels (on rigid models) are not practicable when used on a flexible aircraft. Such calculations should include spanwise, as well as lengthwise, flexibility.

5. *Results of a Stress Analysis.*

After completion of the aeroelastic investigation which has been discussed so far, it was thought wurthwhile to have a brief look into the level of stresses, in order to establish some relationship between strength and stiffness requirements for the narrow delta aircraft. At this stage of the investigation only the order of stress level was required and so several simplifications were made:

(1) Only longitudinal bending was considered.

(2) In the calculations of aerodynamic load distribution the aircraft was assumed rigid but the order of aeroelastic effects on load distribution was considered.

(3) The lengthwise loading distribution considered was that due to aerodynamic lift and corresponding inertia forces. The all-up weight of the aircraft and the weight distribution were kept constant for all skin thicknesses.

Under the above assumptions the bending moment distributions were replotted from Fig. 7 and are again shown in Fig. 12. As the reference point in the calculations was the *CG* at $0{\cdot}635l$, the jump in bending moment due to aerodynamic forces represents the aerodynamic restoring moment. In the dynamic calculations this was balanced mainly by rotary inertia loading and by other aerodynamic loadings such as an m_q contribution. In the present static case this represents an out-of-trim moment which has to be balanced by some form of control force. For the purpose of the present calculations it was assumed that the trimming moment is supplied by a trailing edge control, which was represented by a concentrated force acting at $0{\cdot}95l$. The bending moment distribution obtained is then as shown in Fig. 12 and marked 'trimmed'.

The 'untrimmed' bending moment distribution can be regarded as the distribution due to aerodynamic load when the trimming deflection of the control is instantaneously removed by, for example, a step push

on the control column. In that case however, there is an additional inertia loading due to angular acceleration of the aircraft, which would considerably modify the bending moment distribution basically increasing bending moment in the front part of aircraft and decreasing it at the rear. Thus the values of resultant 'untrimmed' bending moment at the rear of the aircraft can be regarded as an upper limit of bending moment in a transient manoeuvre.

From the bending moments shown in Fig. 12 the maximum stresses were calculated. Of course the longitudinal bending stresses will be greatest at the centre-line of the aircraft. The lengthwise stress distribution in non-dimensional form is shown in Fig. 13. On the right hand side of this figure scales are added which show the stress level in percentage of ultimate for $1g(n = 1)$ load. The ultimate stress was assumed to be 25 tons/sq in. It should be underlined that the stress distribution marked 'trimmed', corresponds closely to level $1g$ flight, and approximates quite well to a steady state pull-out where only the effect of other derivatives such as m_q is neglected.

The mean effect of aeroelasticity would be to increase the aerodynamic loadings at the front of the aircraft and decrease them at the rear, inertia loadings being the same. The overall effect would be an appreciable increase in bending at the front part of the aircraft, but at the rear the effect should be much smaller due to the counter-balancing effect of less control to trim. It is expected that the bending-moment could be easily doubled at the front, but not much change would be expected at the rear.

It should be added that the relatively high stress level near the trailing edge of the aircraft as shown in Fig. 13 is of no practical importance. Firstly, the last 10 per cent of length would be expected to be covered by controls and secondly, the aircraft used in this example has a very hin trailing edge. In addition, the assumed aerodynamic load distribution produces large loads near he trailing edge, conditions which may not be realized in practice.

Taking the above considerations into account it is suggested that the maximum value of non-dimensional stress would be of the order 3×10^{-2} for 'trimmed' flight and of a similar order in 'untrimmed' flight, corresponding to sudden stick application.

When the above value of maximum stress is related to the ultimate stress, it can be seen that even for a skin thickness of 0·25 in. this corresponds to 5 to 6 per cent of ultimate for $1g$ load. This suggests that from a pure strength point of view thicknesses considerably less than 0·25 in. should be sufficient, at least for the configuration considered. On the other hand, from a stiffness point of view as shown in the main part of this report a skin thickness of 0·375 in. may not be sufficient.

6. *Conclusions.*

With regard to dynamic stability the following conclusions may be drawn:

(1) The present, simple approach is sufficiently accurate for the study of large aeroelastic effects.

(2) The aeroelastic effects on the slender delta studied, manifest themselves almost exclusively on the restoring moment.

(3) All aeroelastic effects of a narrow delta are results of rather delicate balance between aerodynamic and inertia forces and of appropriate stiffness distribution.

(4) The very large aeroelastic effects found by Broadbent and confirmed by this analysis are partly due to an unfavourable mass distribution and partly due to unfavourable stiffness distribution.

(5) It is believed that in a real engineering approach the problem of dynamic stability as affected by aeroelastic effects, will be of the same order on a narrow delta aircraft as on any other aircraft of the same size.

(6) There is an indication that although the effects of aeroelasticity on narrow delta stability could easily be made small, the effects on controllability could be severe.

Conclusions arising from the stress analysis are as follows:

(7) It appears that it should be reasonably easy to provide sufficient strength for the narrow delta configuration in flight. The concentrated loads of a conventional undercarriage may well prove to be the main stressing case.

(8) The stiffness requirements have an overriding effect on the structural weight when compared with the strength requirement.

(9) It may be profitable to change our approach to structural design, designing for stiffness and checking for stress, and not the other way round, as is common practice at present.

(10) As the stressing involves close balance of inertia and aerodynamic forces, the so-called static stressing is not possible without detailed knowledge of the aeroelastic properties of the airframe. This points again to the need of starting from stiffness not strength.

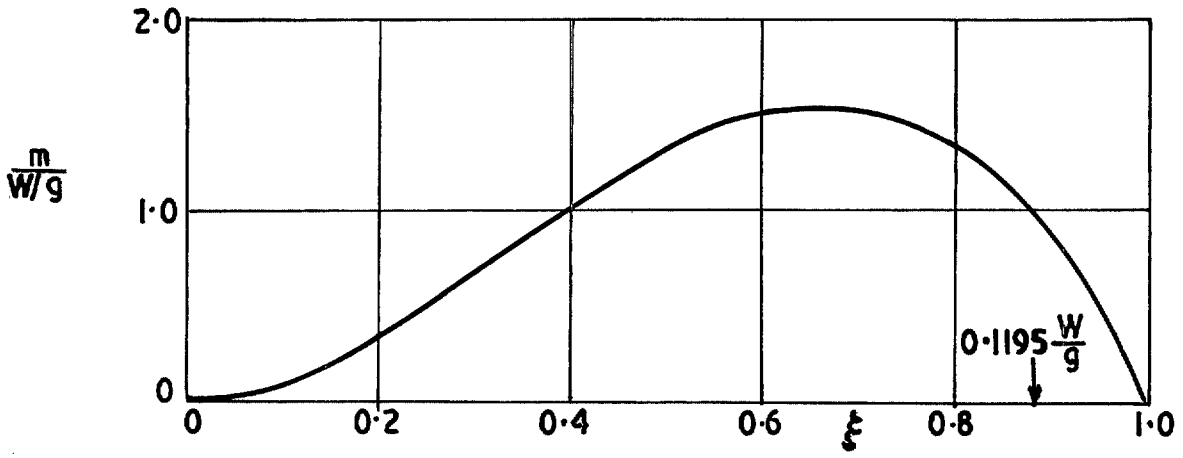

FIG. 1. Longitudinal mass distribution.

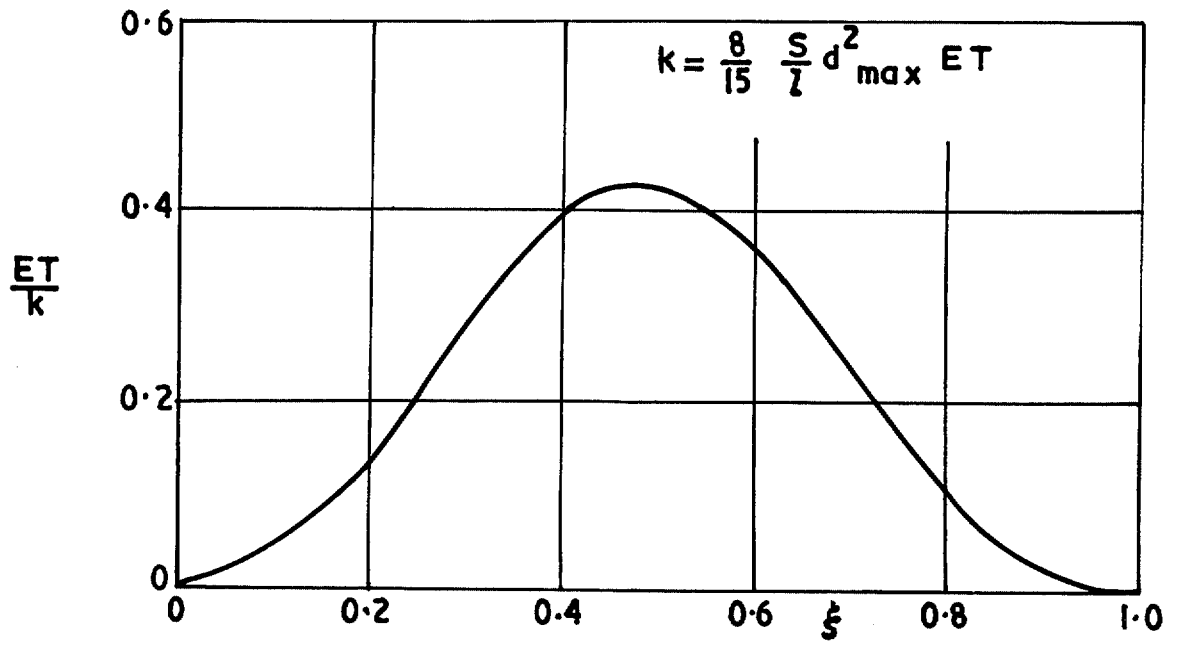

FIG. 2. Longitudinal stiffness distribution.

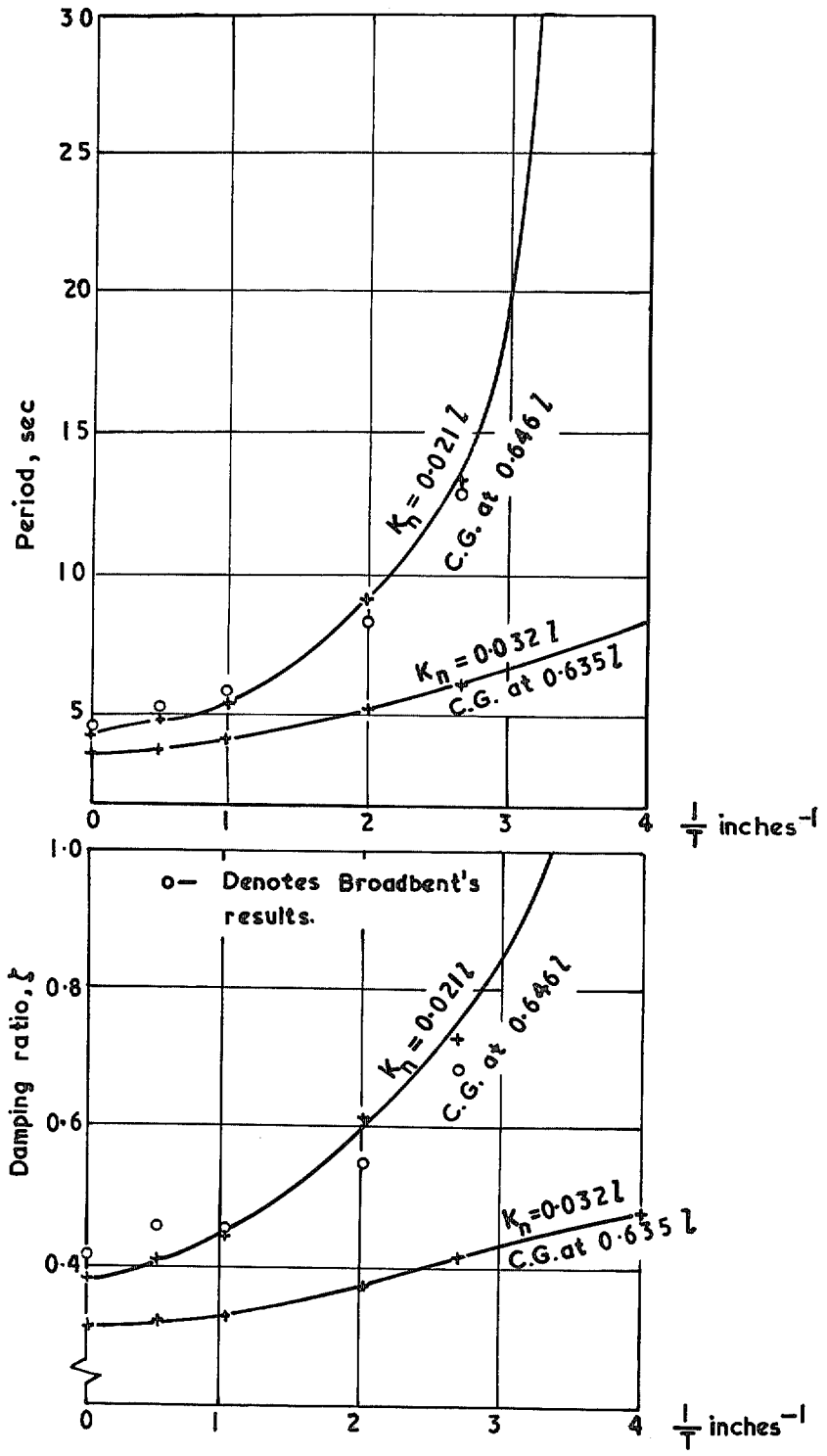

FIG. 3. The effect of flexibility on period and damping of short period mode.

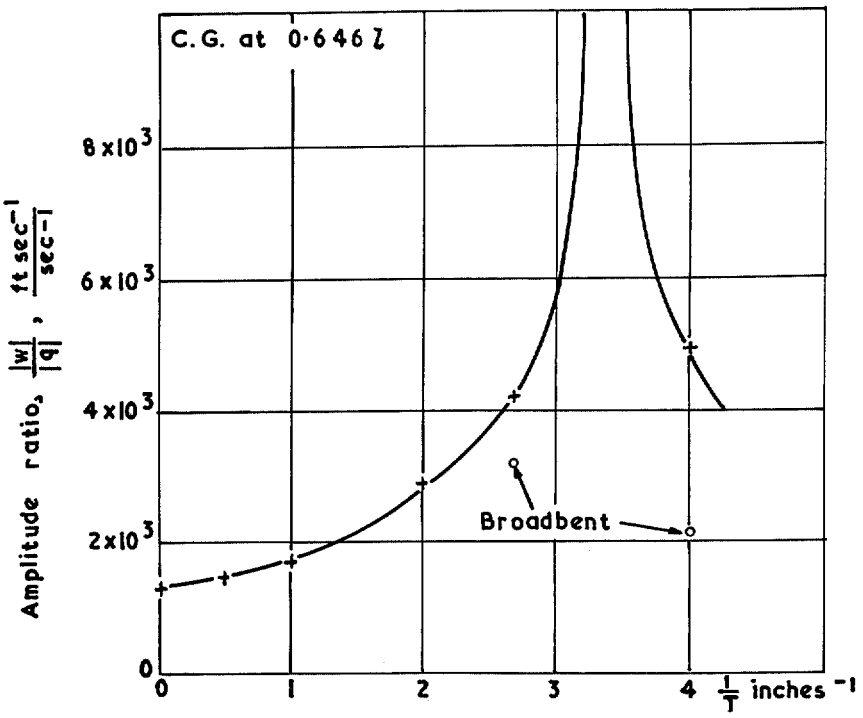

FIG. 4. The effect of flexibility on the amplitude ratio of heaving to pitching.

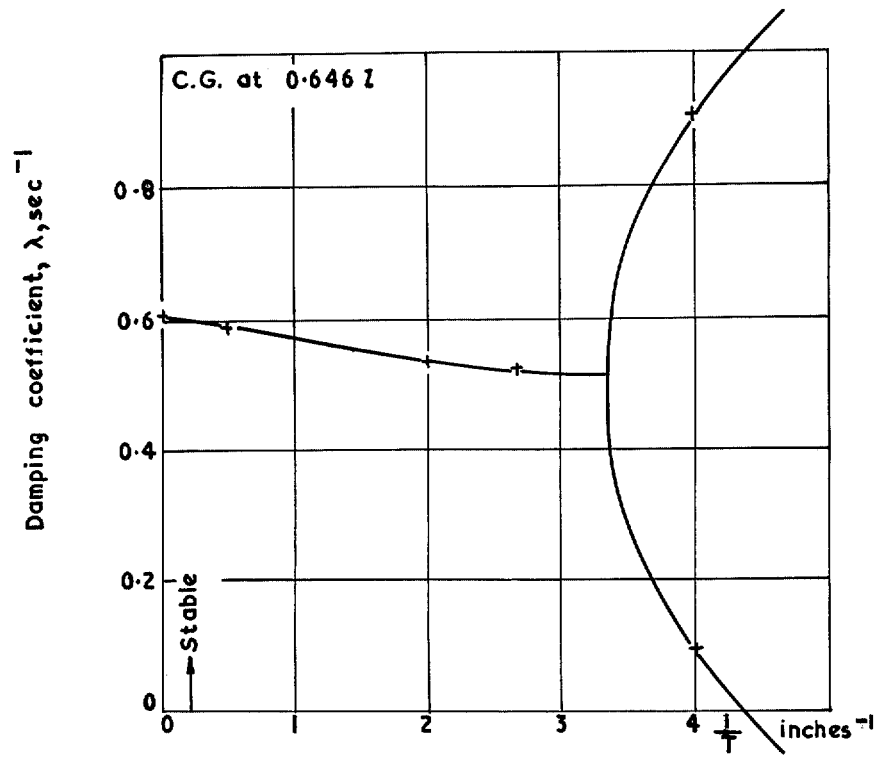

FIG. 5. The effect of flexibility on damping coefficient of the short period mode.

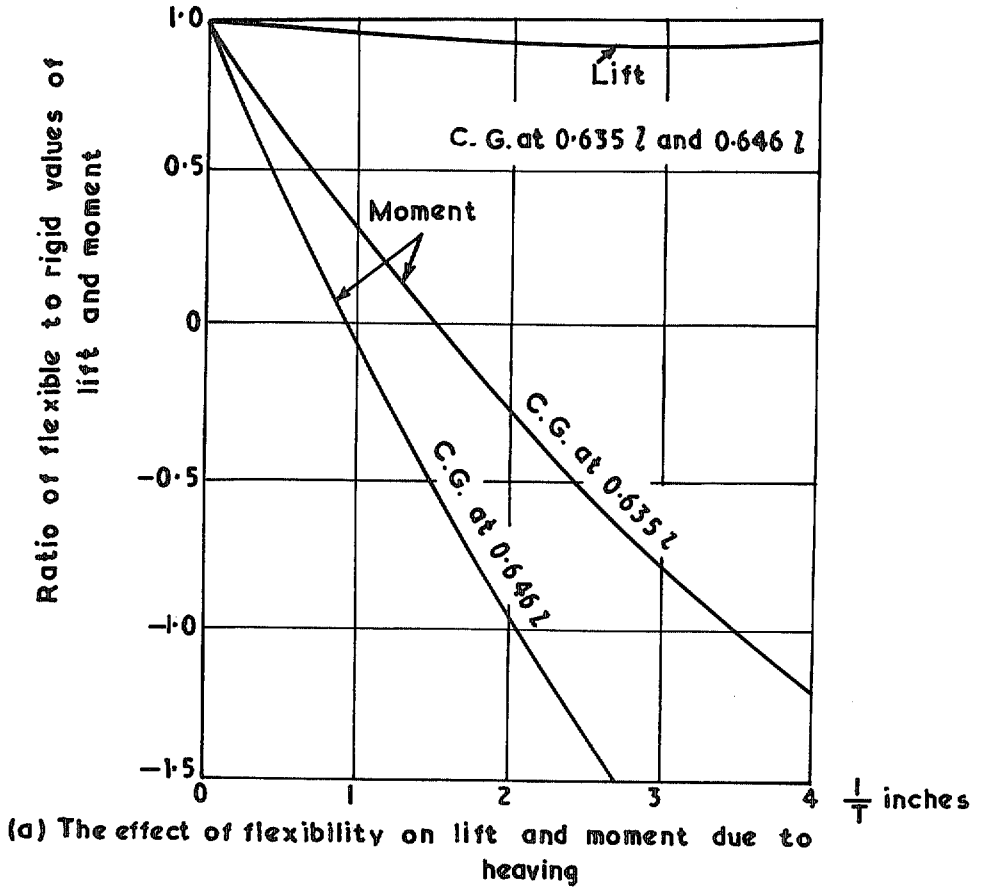

(a) The effect of flexibility on lift and moment due to heaving

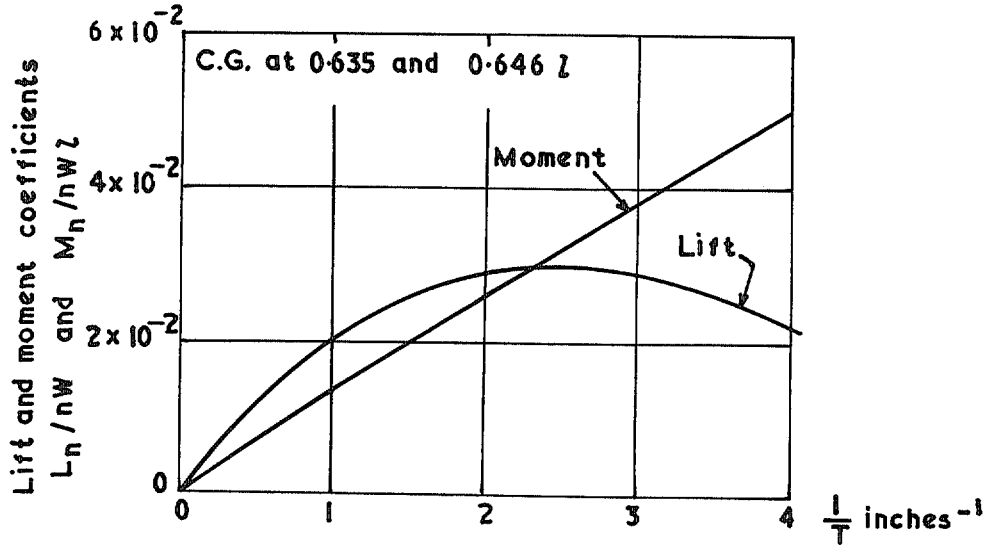

FIG. 6. Some examples of aeroelastic effects.

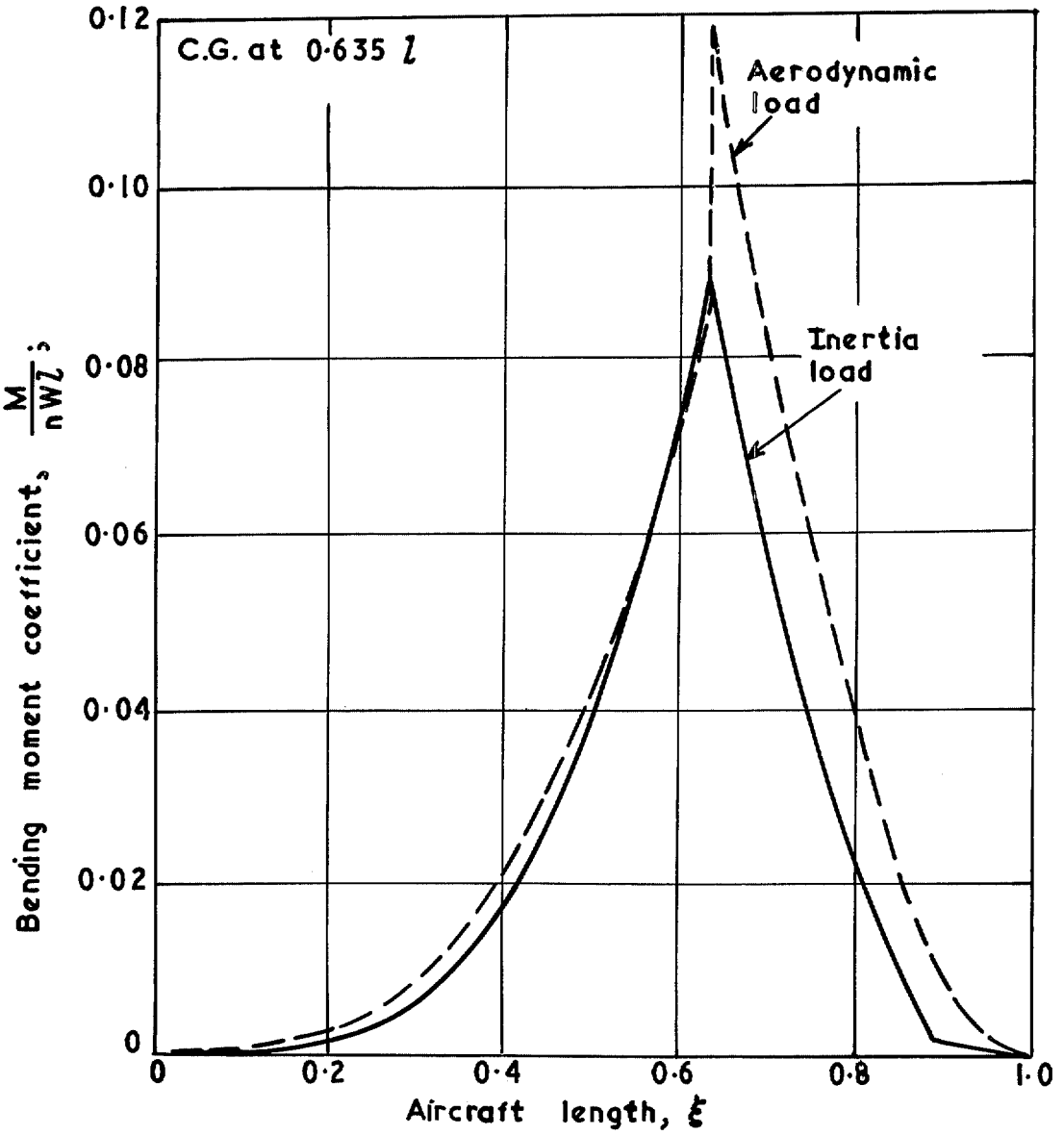

FIG. 7. An example of relative magnitudes of bending moment distribution due to inertia and due to aerodynamic loadings.

(Inertia and aerodynamic loads due to normal acceleration and corresponding incidence $\alpha = \frac{W/S}{aq} n$)

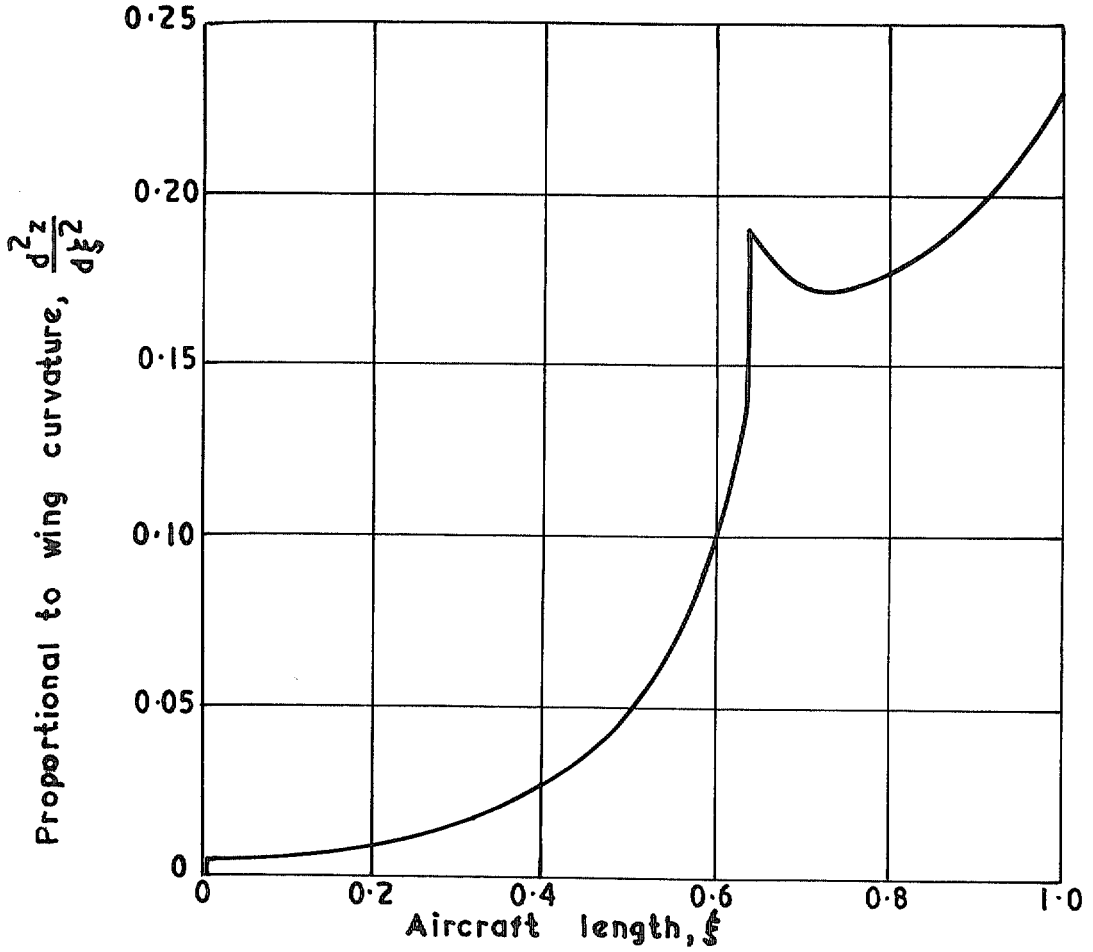

FIG. 8. A typical distribution of wing curvature due to lift.

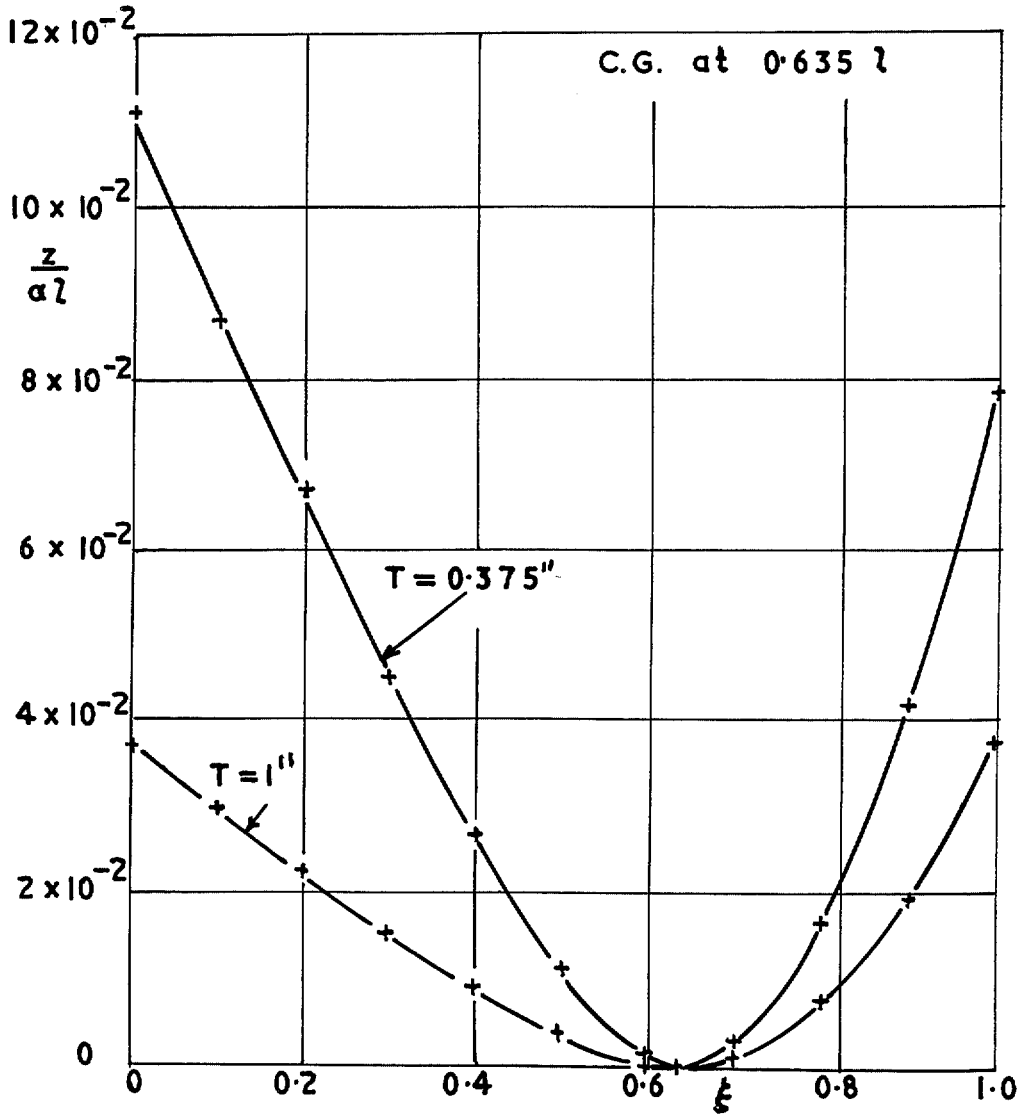

FIG. 9. Deflection due to lift alone.

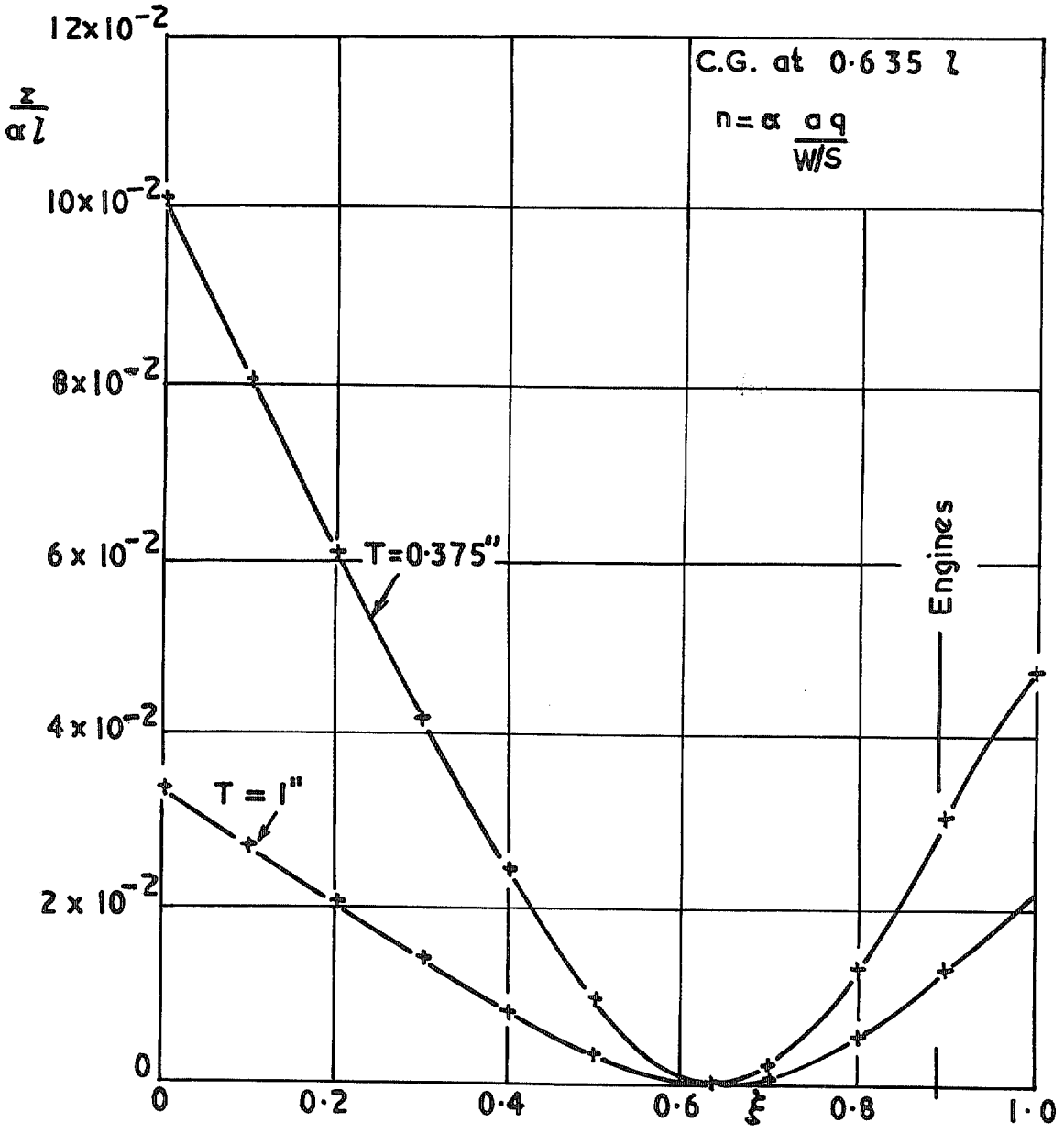

FIG. 10. Deflection due to normal acceleration alone.

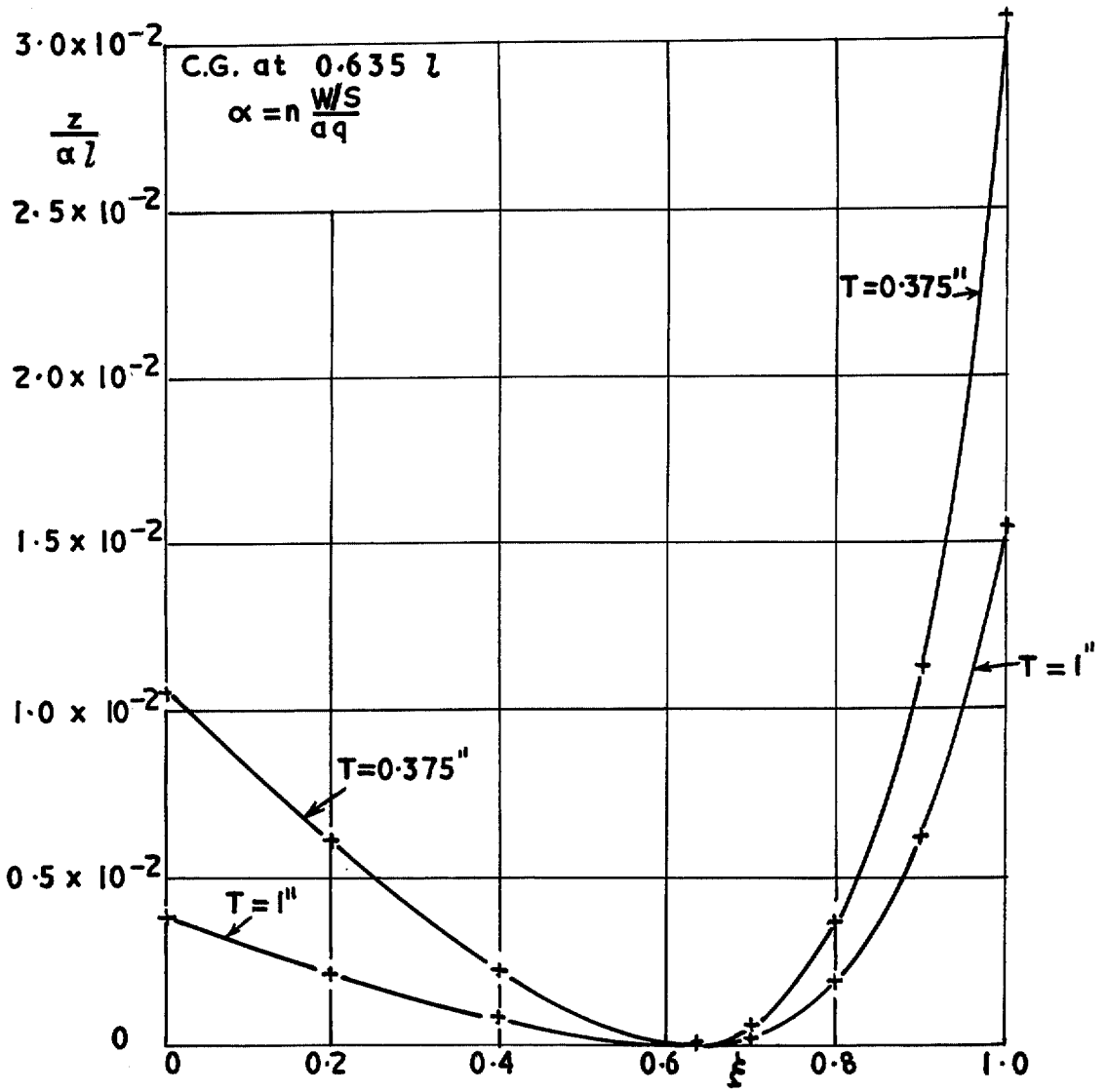

FIG. 11. Deflection due to combined effects of lift and corresponding normal acceleration.

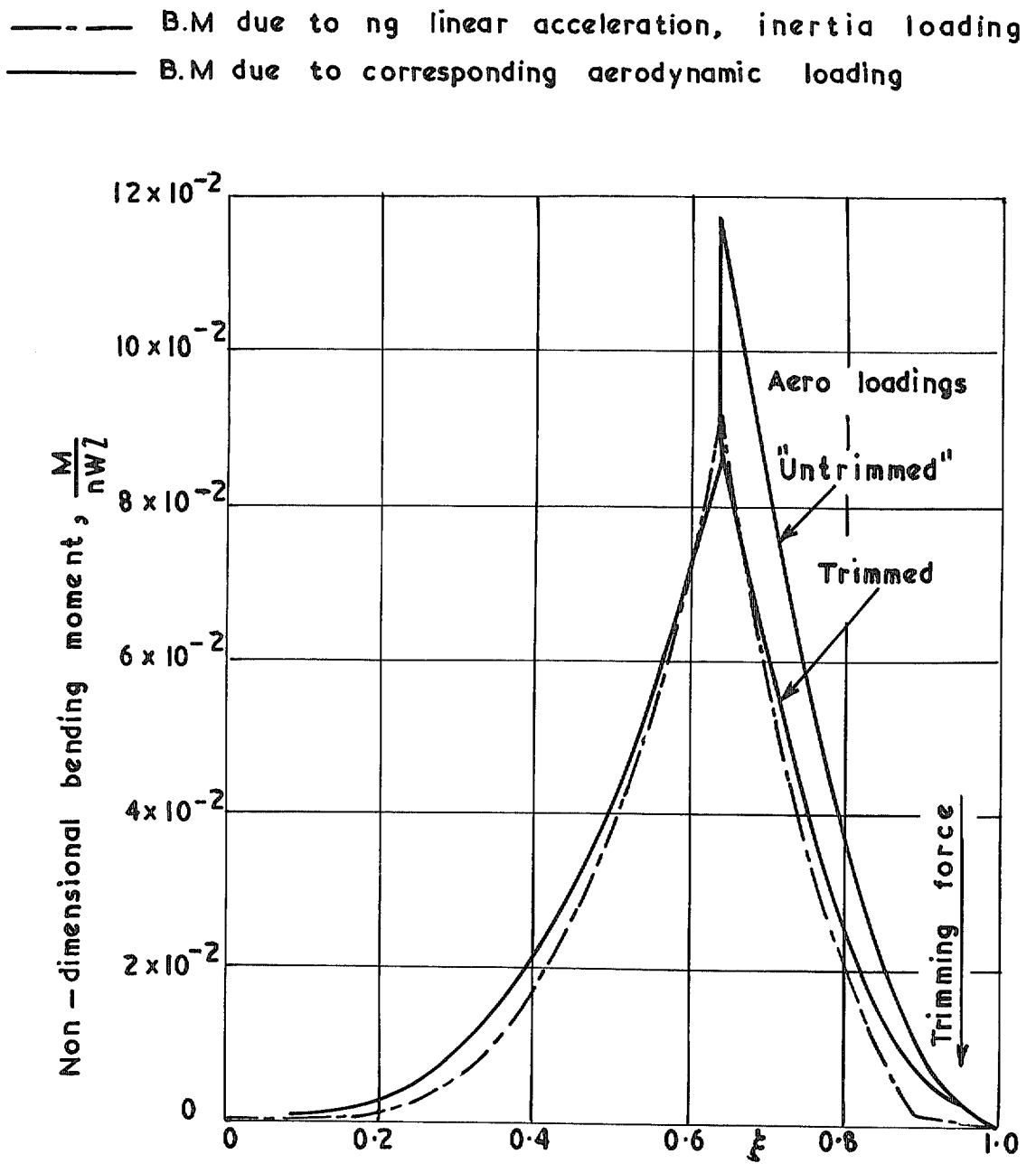

FIG. 12. Lengthwise distribution of rigid body bending moments.

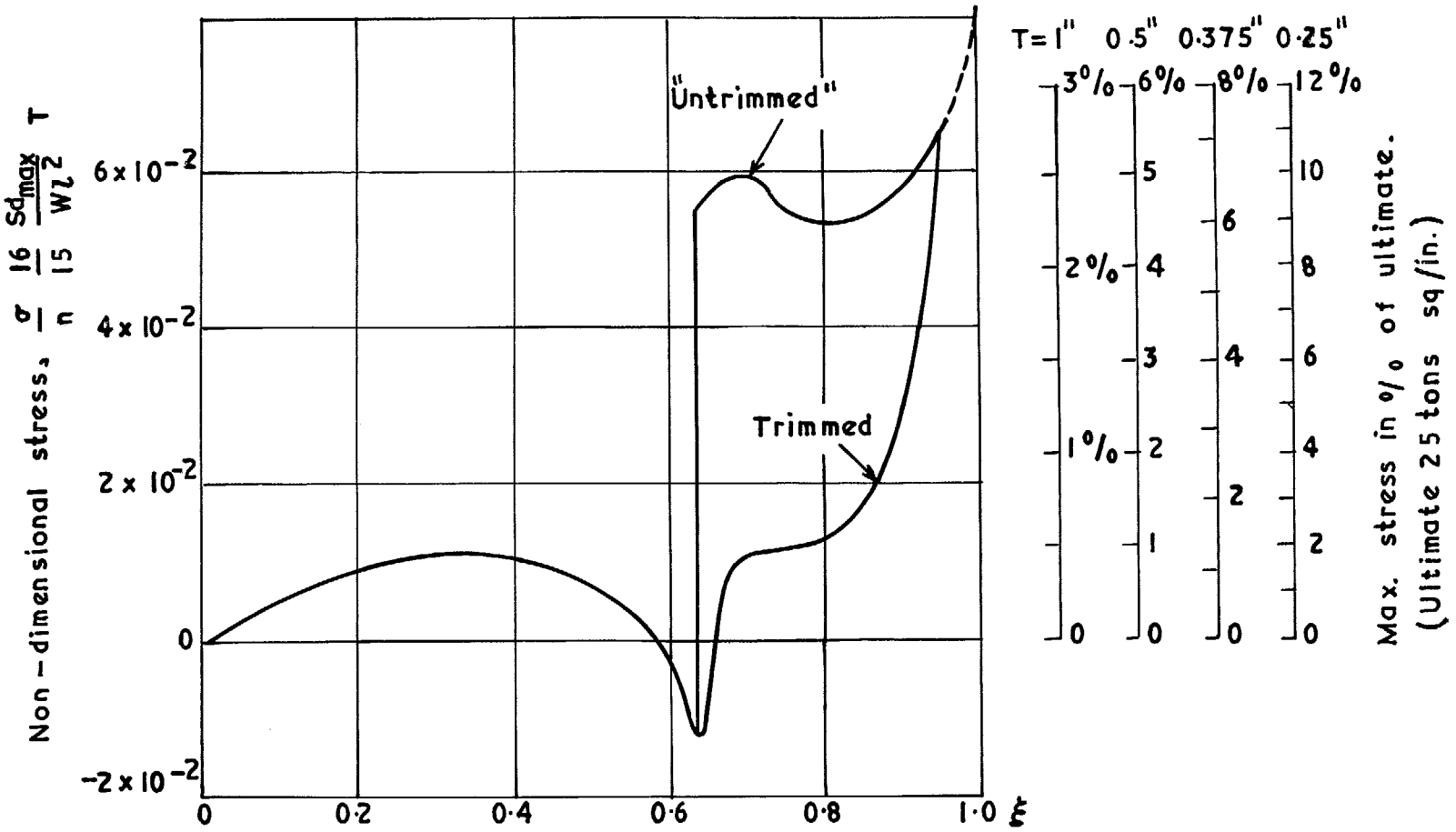

FIG. 13. Lengthwise distribution of maximum bending stress in 1g flight. (Rigid body).

Part III—Dynamic Calculations including Estimates of Elevator Effectiveness

by
J. K. ZBROZEK

1. *Introduction and Assumptions.*

In this report are presented the results of calculations of short period dynamics and response to elevator deflection. The analysis is very simplified but it is thought to make some contribution to the better understanding of the dynamic and aeroelastic properties of slender wings. It is assumed that the aircraft response in the pitching plane can be approximated by three modes, namely, the two rigid body modes in heaving and pitching and one structural normal mode in longitudinal bending. The rest of the assumptions are the same as those made previously. As before two static margins are considered: 0·021l, corresponding to a CG position of 0·646l, and 0·032l. For the latter it is assumed that structural and aerodynamic derivatives other than m_w are the same as for a static margin of 0·021l.

The same assumptions are made regarding wing depth distribution and bending stiffness distribution (Figs. 1 and 2 of Part II). The size and position assumed for the elevators are shown in Fig. 1, the ratio S_n/S of elevator to wing area being 0·115. In the response to elevator calculations, the elevator was assumed not to alter the elastic properties as defined by the first normal mode (Fig. 2). Thus the calculations over-estimate elevator effectiveness as they do not take into account, for example, elevator and wing twist.

The first normal mode was calculated by a method of successive approximations, the first guessed mode shape being that obtained for static deflection obtained in the quasi-static calculations. The final mode shape which satisfies the equation

$$\frac{d^2}{dx^2}\left[EI\frac{d^2w_1}{dx^2}\right] = m\omega_1^2 w_1$$

is shown in Fig. 2. The corresponding frequency is given by

$$\omega_1^2 = 153\frac{g\,d_{\max}^2}{(W/S)l^4}ET\,.$$

This gives

$$\omega_1^2 = 480T\ (T \text{ being in inches})$$

upon substituting the values $g = 32{\cdot}2$ ft sec^{-2}, $W/S = 69{\cdot}5$ ft^{-2},

$$d_{\max} = 12 \text{ ft}, \quad l = 226{\cdot}8 \text{ ft}, \quad E = 15\times10^8 \text{ lb ft}^{-2}\,.$$

2. *Results and Discussion.*

2.1. *Short Period Mode Frequency and Damping.*

The results of calculations for $K_n = 0{\cdot}021$ are presented in Fig. 3, where period and damping ratio of the short period oscillations are plotted against the reciprocal of skin thickness. The results of Parts I and II are also included. It can be seen that the numerical agreement between the present and previous calculations is surprisingly good, bearing in mind the very crude representation of airframe elastic properties. This is probably due to very small spanwise distortions in the first true fundamental

mode and also due to relatively small contributions of the other elastic modes to the short period characteristics.

Fig. 4 shows the total damping of the short period oscillations and indicates that the present calculations predict instability if the skin thickness is reduced below a certain value. The instability is again a pure divergence, due to the manoeuvre margin becoming zero because of aeroelastic effects. It should be remembered that the results apply only for a static margin of $0{\cdot}021l$. By increasing the static margin by 50 per cent to $0{\cdot}032l$ the problem of aeroelastic effects is substantially reduced as may be seen in Fig. 8.

2.2. *Elevator Effectiveness.*

Let us first consider the definition of elevator effectiveness. One possible definition is the change in pitching moment per unit of elevator deflection. However, such a definition is not entirely unique when applied to the elastic airframe. Defining the effective elevator power, including aeroelasticity, we must also specify the restraint which is necessary to balance the pitching moment of the elevator. On a conventional aeroplane, where the aeroelastic distortions are mainly those of the tailplane with elevator, and of the rear part of the fuselage, the usual approach is to fix the fuselage at the aircraft CG and consider the distortions of the rear fuselage and empennage. A similar approach was used by W. G. Molyneux in some unpublished work on a configuration similar to the one used in the present report and it was found that the elevator effectiveness (i.e. the pitching moment with respect to the CG of the aircraft restrained in pitch) falls to zero at a skin thickness of $T = 0{\cdot}085$ in. $(1/T = 11{\cdot}76)$.

A second possible definition of the elevator effectiveness is the amount of normal acceleration per unit elevator deflection. This definition includes the aeroelastic and dynamic properties of the whole aircraft. This approach has been used in the present calculations giving the results shown in Figs. 5 and 6. Denoting elevator effectiveness by n/η, expressed in g units per degree, we can define relative effectiveness as the ratio of the flexible aircraft value of n/η to the rigid aircraft value (the latter corresponding to $1/T = 0$). The relative effectiveness is shown in Fig. 5 plotted against $1/T$ for static margins of $0{\cdot}021l$ and $0{\cdot}032l$.

The estimated values of 'g' per elevator angle for the rigid aircraft are:

$$n/\eta \simeq -0{\cdot}8 \text{ per degree for } K_n = 0{\cdot}021l$$

and

$$n/\eta \simeq -0{\cdot}5 \text{ per degree for } K_n = 0{\cdot}032l\,.$$

The definition of elevator effectiveness as acceleration per degree of elevator deflection reveals, at first sight, a rather unexpected effect of flexibility for reducing skin thickness actually increases the effective elevator power. This phenomenon is due to the fact that reducing the airframe stiffness decreases the manoeuvre margin more rapidly than it reduces the elevator pitching moment per degree. This point is more clearly illustrated in Fig. 6 where the relative elevator effectiveness is plotted against $1/T$ for a wide range of airframe stiffness for three values of the rigid aircraft static margin. It can be seen that for the two smaller values of the static margin, reducing the airframe stiffness increases relative effectiveness which approaches an infinitive value when the manoeuvre margin approaches zero. For a still more flexible airframe it reverses sign, becoming negative, and becomes zero at some quite small skin thickness (0·119 in. for $K_n = 0{\cdot}032l$ and 0·093 in. for $K_n = 0{\cdot}021l$). Reducing the skin thickness yet further restores the positive elevator effectiveness, because the manoeuvre margin and 'true' elevator power are both negative.

For $K_n = 0{\cdot}05l$, the largest value of the static margin considered, it was estimated that the manoeuvre margin should vanish for $1/T \simeq 9$; thus it was expected that the elevator power (pitching moment) would decrease faster with decreasing skin thickness than the manoeuvre margin. The calculations of the relative elevator effectiveness shown in Fig. 6 confirm this expectation. For this value of the static margin, decreasing the skin thickness decreases the relative effectiveness and a zero value is reached for $T \simeq 0{\cdot}185$ in.

It can be concluded that the term 'elevator effectiveness' when applied to an elastic aircraft requires careful definition. It has been shown by the present calculations that the effect of elasticity on the relative effectiveness is not only a function of the elevator power but can also be a function of the static margin of the rigid airframe. We have here a situation similar to that for the lateral response to aileron. The stiffness at which the manoeuvre margin vanishes corresponds to the divergence speed, and the stiffness at which the elevator power vanishes corresponds to the reversal speed. The main difference is the difficulty of defining the elevator-alone power due to lack of an easy definition of the restraint.

To illustrate further the problem of the definition of elevator power, the relative effectiveness was calculated neglecting both rigid body modes. The results are shown in Fig. 6 as a curve labelled 'elevator-alone effectiveness'. The physical interpretation of such calculations, which take into account only the elastic mode, is rather difficult. It can be said that this 'elevator-alone effectiveness' is the effectiveness of elevator on an elastic airframe constrained at the nodal points. There is very little physical significance in such a definition.

A similar method was used by Molyneux in the work referred to earlier in which the elevator pitching moment with respect to the *CG* was calculated for an elastic airframe (analysed by six arbitrary modes) restrained at the *CG*. Molyneux predicted zero elevator effectiveness at $T = 0{\cdot}085$ in. From Fig. 6 we see that the curve for 'elevator-alone effectiveness' in the present case falls to zero at $T = 0{\cdot}115$ in. This apparently reasonable agreement is however of little consequence since the results depend upon the assumptions about the restraint; these assumptions differ in the two cases and in each case have little physical significance.

2.3. *The Structural Mode Frequency and Damping.*

The frequency and damping of the structural mode, as affected by aerodynamic forces and by coupling with rigid body are shown in Fig. 7. It may be seen that coupling with the rigid body modes increases very slightly the frequency and increases somewhat the damping. The results are almost identical for the two values of static margin considered.

2.4. *The Effects of Static Margin.*

The effects of flexibility on the period and damping of the short period oscillation for two values of rigid body static margin are shown in Fig. 8. The results are very similar to those obtained in Part II, and demonstrate again that the loss in stability is mainly due to the reduction in manoeuvre margin with decreasing airframe stiffness.

2.5. *The Effect of Engine Thrust.*

The present approach makes possible a simple assessment of the engine thrust effect. It is assumed that the engine thrust acts tangentially to the airframe deflection at the engine *CG*, i.e. at $\xi = 0{\cdot}889$. Under this assumption the engine thrust produces destabilising lift and pitching moment increments in phase with the structural mode deflection. These increments of lift and moment are small compared with the lift and moment due to elastic distortion, and thus the destabilising effect of engine thrust was expected to be small. This was checked and confirmed by numerical calculations. They showed that the engine thrust reduced the manoeuvre margin further but the numerical values computed were within a few per cent of those which neglected engine thrust.

3. *Concluding Remarks.*

The results presented here provide a very rapid and easy to grasp physical picture of the dynamic properties of an elastic airframe. The main difficulty was to establish the normal mode shape and frequency. It was found, however, that starting with a good guess of the modal shape, the normal mode could be reasonably quickly established through only a few successive approximations in an attempt to satisfy the free-free beam equation.

The present study leads to conclusions somewhat contradictory to those of Part II. There it was stated that '(3) All aeroelastic effects on a narrow delta are results of rather delicate balance between

aerodynamic and inertia forces and of appropriate stiffness distribution'. and '(4) The very large aeroelastic effects found by Broadbent and confirmed by this analysis are partly due to an unfavourable mass distribution and partly due to an unfavourable stiffness distribution.'

The present study shows that the loss of longitudinal stability can be quite satisfactorily explained by the aerodynamic moments arising from aeroelastic distortions defined by just one fundamental chordwise bending mode. This mode is a basic property of a long beam, which the narrow aircraft actually is, and no changes in mass or stiffness distribution can alter fundamentally the shape of this mode. Further, the wing area is distributed along this beam, so that whatever the aerodynamic theory and the aerodynamic load distribution assumed, the airframe deflection in its fundamental mode will always produce a large pitching moment. There are only three ways of reducing this destabilising aeroelastic effect. The first is to have initially large stability (as a rigid body) so that any losses due to elasticity are comparatively small. This is demonstrated in both Parts II and III. The second is to reduce the magnitude of aeroelastic distortions and hence effects by increasing the stiffness. The third is to decrease the coupling between the rigid body and elastic modes. For example the excitation of the structural, fundamental bending mode could be considerably reduced by decreasing the wing area outside the nodal points, and increasing it in between the nodal points. This of course brings us back again to the problem of 'careful balance between the inertia, aerodynamic and stiffness forces'.

The above argument leads to the much broader conclusion that any aeroplane which structurally can be approximated by a long slender beam and has a lifting surface distributed (not necessarily continuously) along this beam, will suffer from earoelastic problems akin to those discussed in the present paper.

It is difficult to define the elevator effectiveness on an aircraft with large aeroelastic effects. It is suggested that the only unambiguous definition is in terms of the steady state aircraft acceleration response per unit of elevator deflection. It is felt that this definition should be satisfactory even when transient responses are considered, for example the pitching acceleration due to abrupt deflection of elevator.

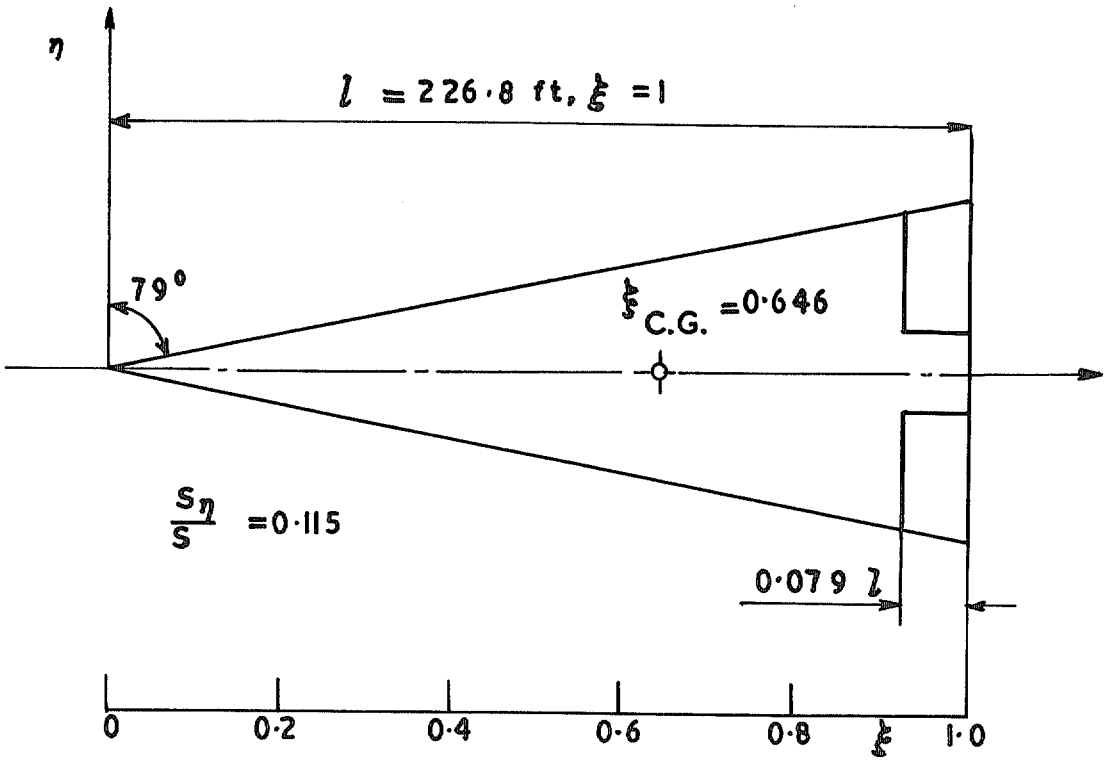

FIG. 1. Wing and control planform.

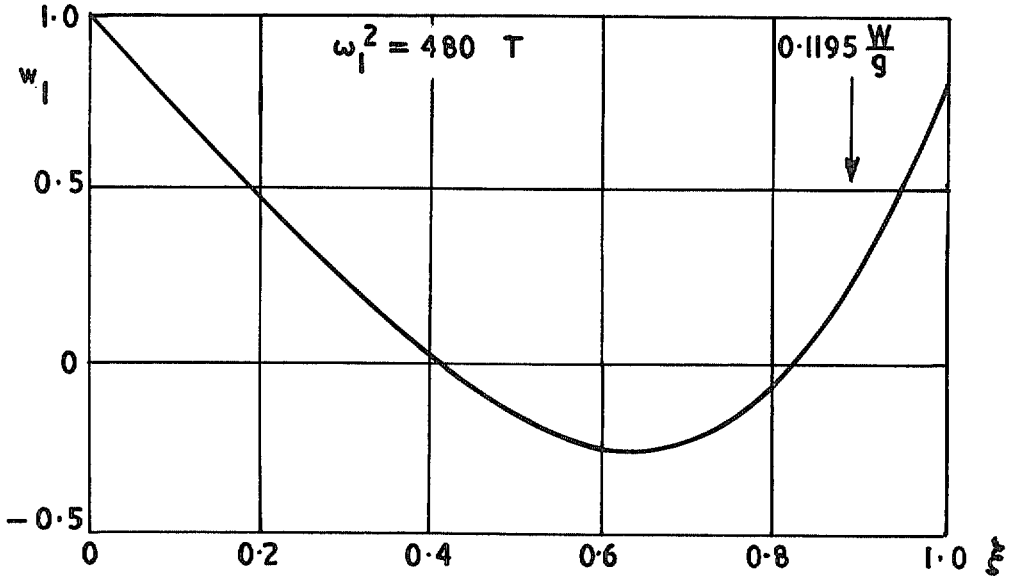

FIG. 2. Estimated first normal mode.

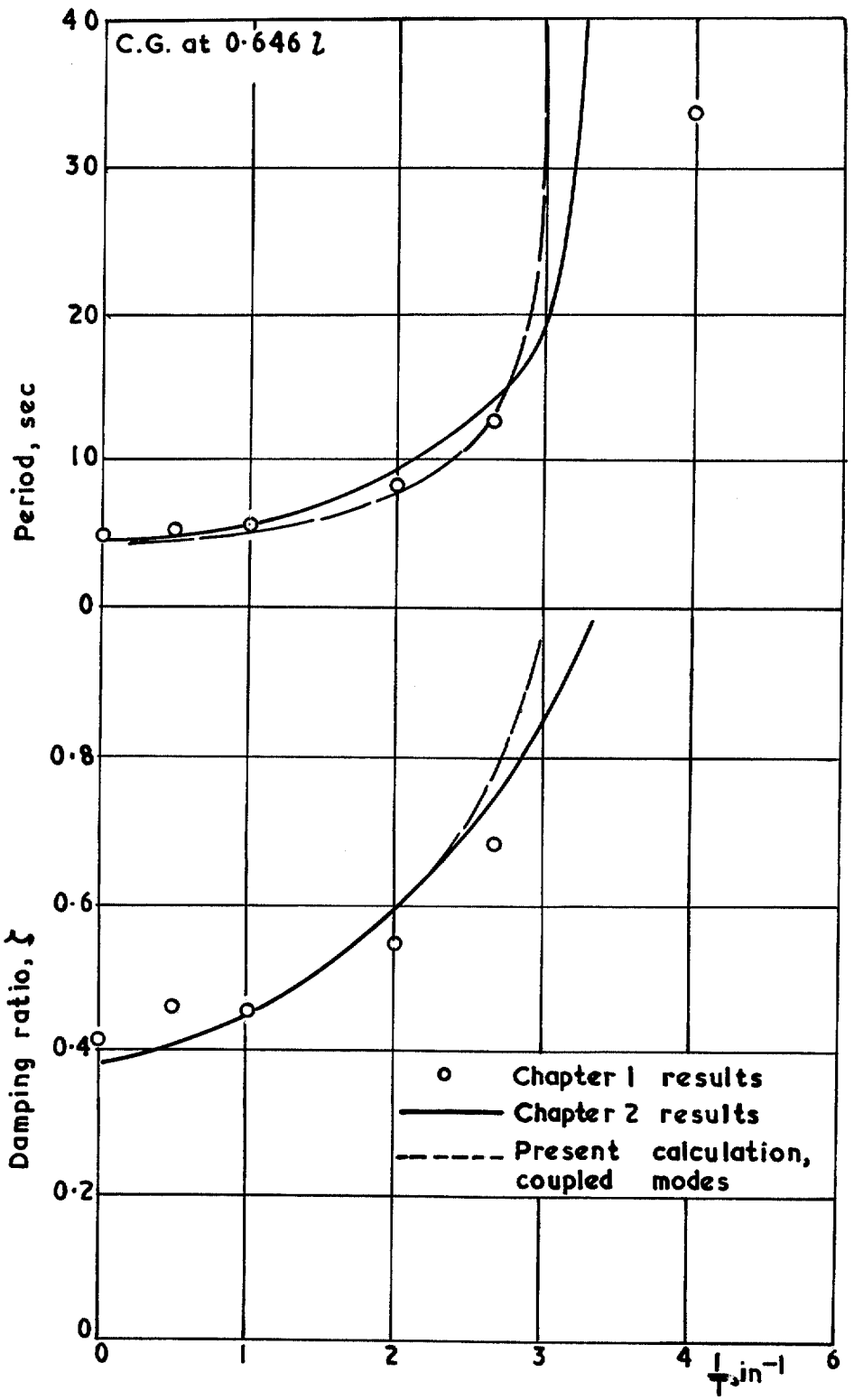

FIG. 3. The effect of structural stiffness on period and damping of short period mode. A comparison of three methods of analysis.

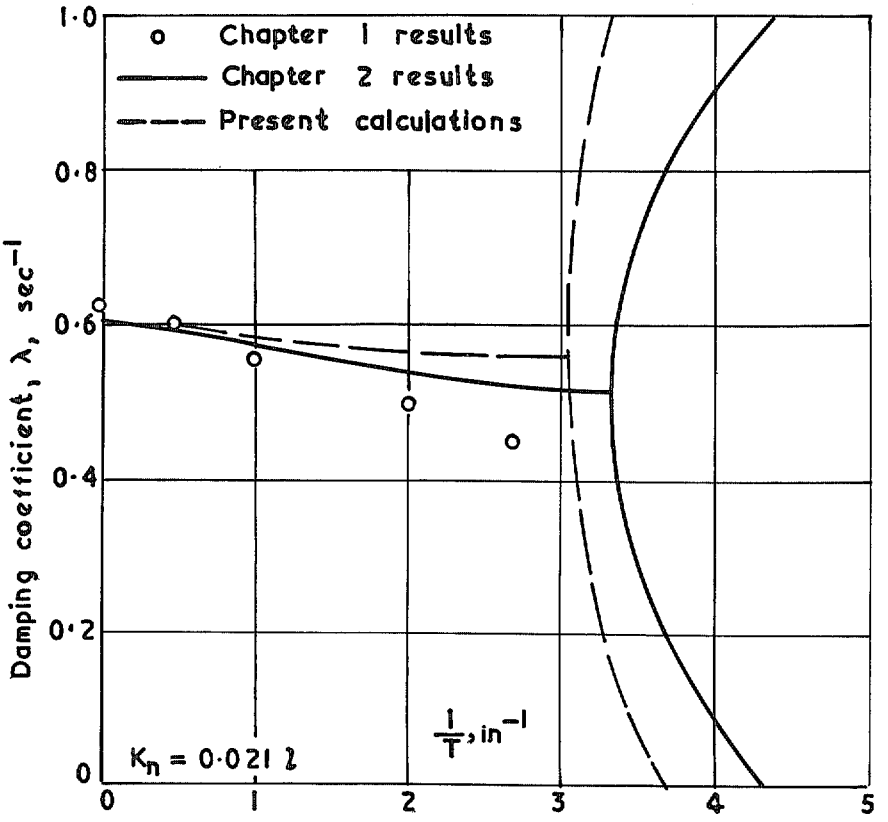

FIG. 4. The effect of flexibility on damping coefficient of short period mode.

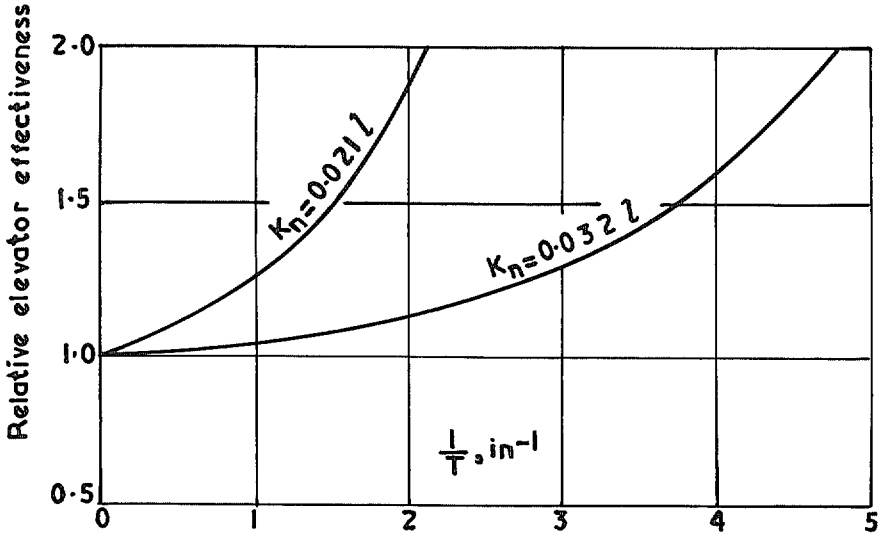

FIG. 5. The effect of flexibility on elevator effectiveness.
(In terms of "g" per η).

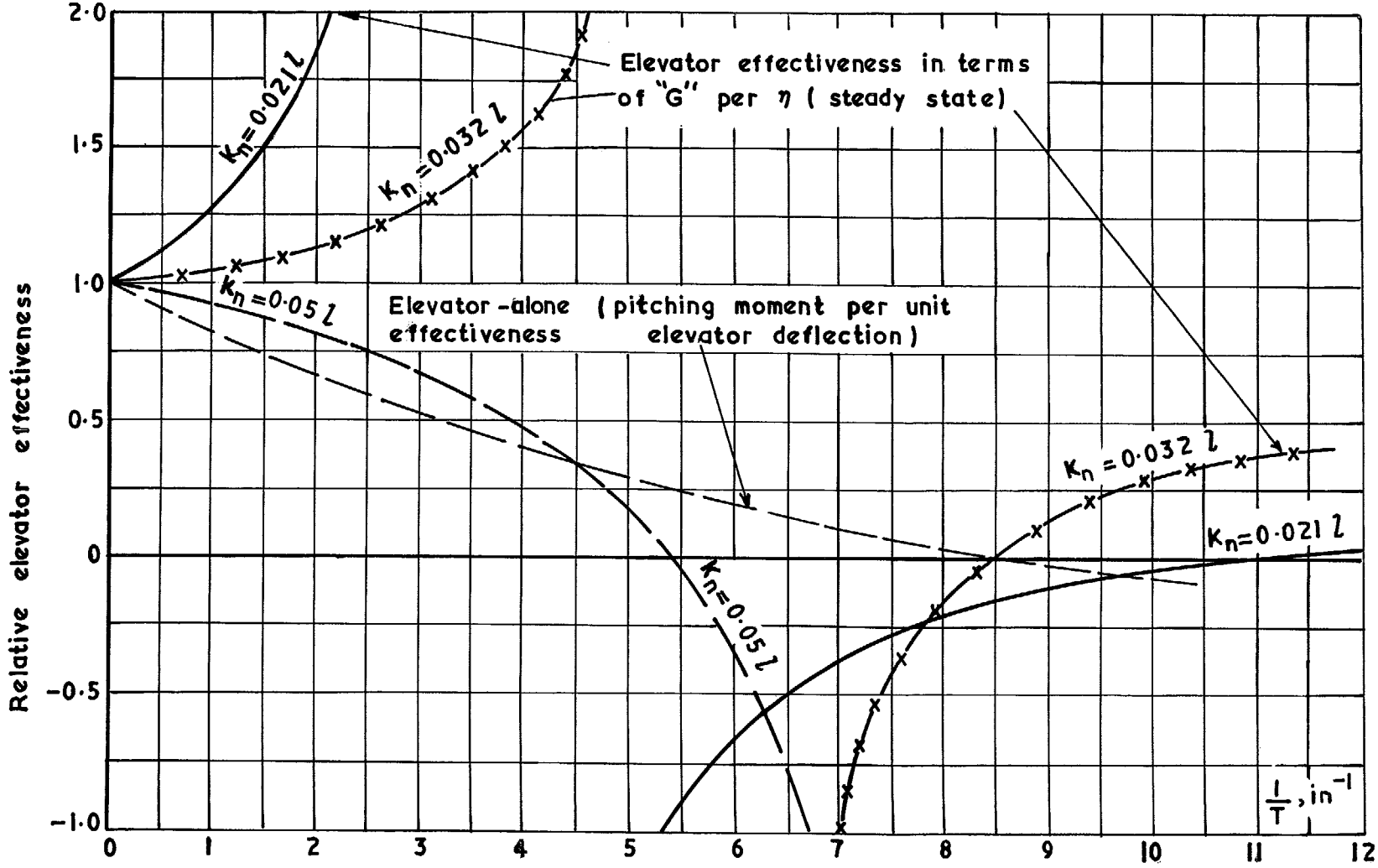

FIG. 6. The effect of flexibility on elevator effectiveness for three values of static margin. Comparison of two definitions of elevator effectiveness.

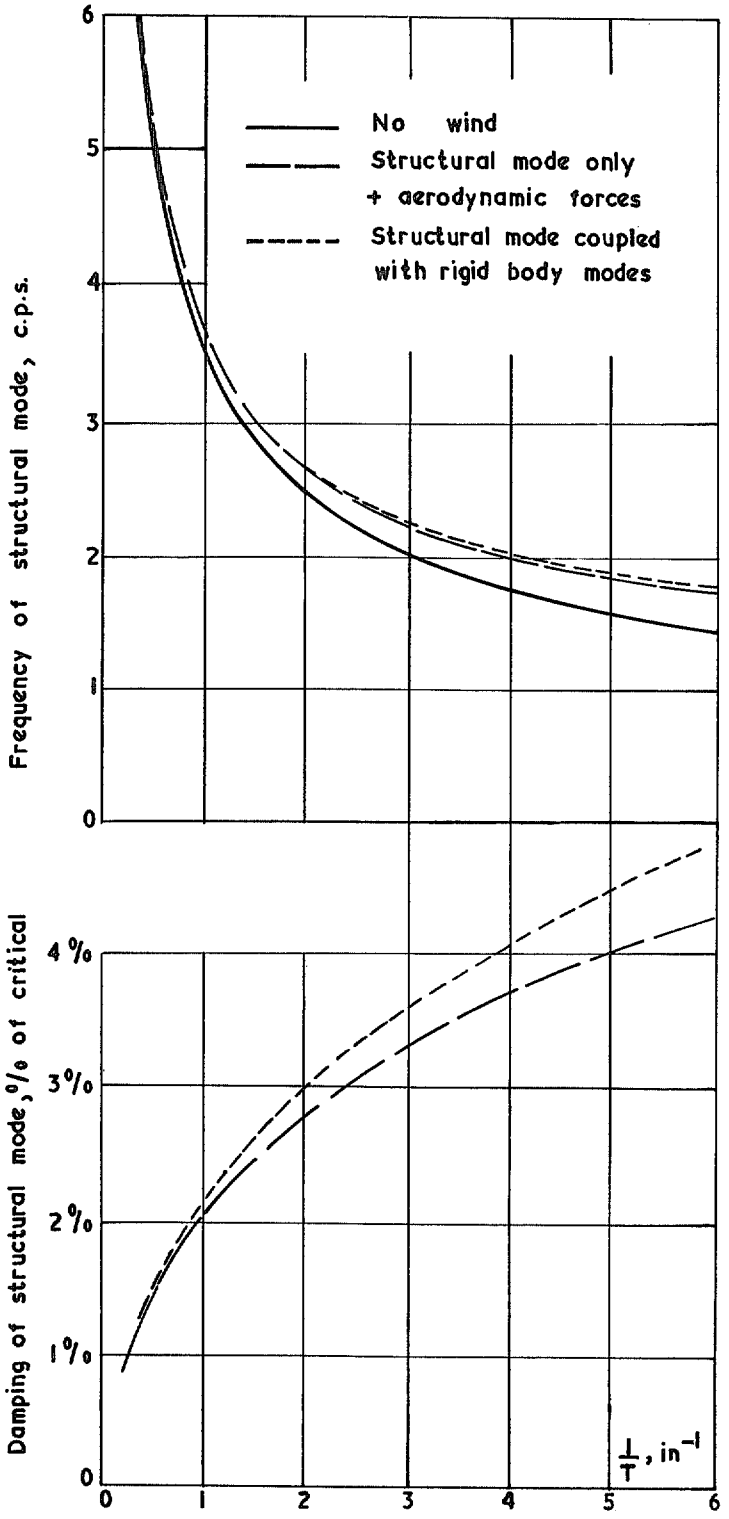

FIG. 7. Frequency and damping of structural mode against reciprocal of skin thickness. The effect of aerodynamic forces and of coupling with rigid body modes.

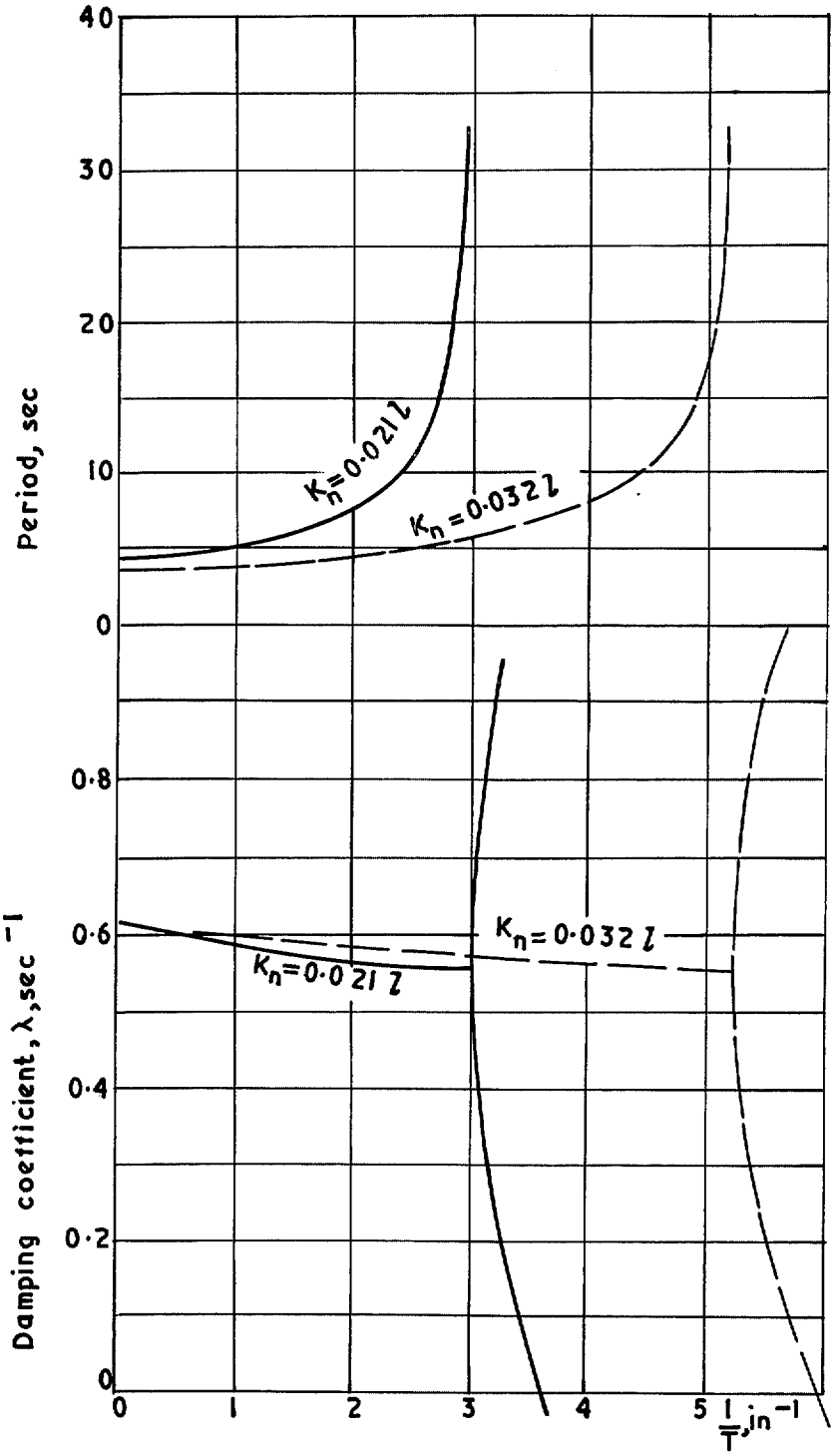

FIG. 8. The effect of flexibility on period and damping of short period mode for two values of static margin.

Part IV—Calculations of the Bending Response to Discrete Vertical Gusts

by
E. HUNTLEY

1. *Introduction.*

Once it was clear that the model set up by Zbrozek was adequate for a study of the dynamics of a slender flexible aircraft it was decided that the next important problem to be studied should be the question of the bending response to air turbulence. A complete analysis would have been extensive since it should have included aircraft responses in pitch, heave and perhaps several bending modes, the effect of skin thickness and various types of gust input including both discrete gusts and continuous random turbulence. In this chapter only part of the problem is studied since the aircraft is assumed to respond only in heave and longitudinal bending in the first normal mode, the skin thickness is kept constant at 0·375 in. and only step and ramp-type vertical gusts are considered. [Further work has been done subsequently on the responses of the same slender aircraft to random turbulence by Zbrozek[1] and Huntley[2]].

2. *Assumptions and Equations of Motion.*

The same idealised slender delta aircraft studied by Broadbent and Zbrozek is used for the present calculations. The aircraft is assumed to be flying at $M = 2{\cdot}0$ at 40 000 ft and to have a lift curve slope of 2·0. The response to a step gust is derived considering only heave and longitudinal bending in the first normal mode, pitching and any other bending modes, longitudinal or transverse, being neglected. The gust loads are assumed to act instantaneously at each station as the gust front passes it and neither Küssner nor Wagner effects are included. The aerodynamic loads are estimated by piston theory so that at any point they are taken to be proportional to the instantaneous incidence of the wing surface at that point.

The bending moment equation is formulated by considering the general equation for forced vibration of a beam by a forcing function $F(x, t)$ and neglecting structural damping

$$\frac{\partial^2}{\partial x^2}\left(EI(x)\frac{\partial^2 Z}{\partial x^2}(x,t)\right) = -m(x)\frac{\partial^2}{\partial t^2}Z(x,t)+F(x,t)\,.$$

This is solved by using the natural modes of vibration of the wing, i.e., by assuming a solution of the form

$$Z(x,t) = \sum_i z_i(t)\, w_i(x)$$

where $w_i(x)$ is the mode shape satisfying the equation for free vibration in the i^{th} mode

$$\frac{d^2}{dx^2}\left(EI\frac{d^2 w_i}{dx^2}\right) = m\,\omega_i^2\, w_i\,,$$

and the orthogonality conditions

$$\int_0^l m\, w_i\, w_j\, dx = 0 \text{ for } i \neq j$$

and $$\int_0^l m w_i^2 \, dx = M_i$$

where M_i is the generalised mass in the i^{th} mode. This leads to the following ordinary second order equations for the $z_i(t)$.

$$(\ddot{z}_i + z_i \omega_i^2) M_i = F_i$$

where $F_i = \int_0^l F w_i \, dx$ is the generalised force in the i^{th} mode.

Since, in the present case, all bending modes other than the first mode are neglected, a solution of the form.

$$Z(x, t) = z_o(t) w_o(x) + z_1(t) w_1(x)$$

is assumed. $i = 0$ corresponds to the heaving mode with $\omega_o = 0$ and $i = 1$ to the first bending mode. $w_1(x)$ had been established by Zbrozek by the method of successive approximations and is shown in Fig. 2, of Part III, the frequency of the mode ω_1 being given by $\omega_1^2 = 480T$. The generalised force in the first mode, F_1, includes aerodynamic terms from the heaving mode and aerodynamic stiffness and damping terms from the bending mode itself.

Details of the derivation of the equations of motion of the aircraft are given in Ref. 2. The lift equation is taken to be that normally used when considering the short period motion of a rigid body together with additional terms due to the bending mode. The resulting equations in true time for heaving (1) and bending (2), are

$$(D + \frac{a}{2\hat{t}})w - \frac{a}{\hat{t}}\left(0{\cdot}0406D + 0{\cdot}6256\frac{V}{l}\right)z_1 = -\frac{L_g(t)}{\rho V S \hat{t}}, \tag{1}$$

$$-w + 1{\cdot}414\frac{\hat{t}}{a}\left[D^2 + 0{\cdot}887\frac{a}{\hat{t}}D + \left(4{\cdot}415\frac{V}{l}\frac{a}{\hat{t}} + \omega_1^2\right)\right]z_1 = \frac{F_{1g}(t)}{0{\cdot}0406\,\rho V S a}. \tag{2}$$

The lift due to a 1 f.p.s. vertical gust can be expressed analytically in terms of a non-dimensional gust penetration parameter $\xi_1 = \left(\frac{Vt}{l}\right)$,

$$\frac{L_g(t)}{\rho V S \hat{t}} = \frac{a.}{2\hat{t}}\xi_1^2 \qquad 0 \leqslant \xi_1 \leqslant 1{\cdot}0$$

$$= \frac{a}{2\hat{t}} \qquad 1{\cdot}0 \leqslant \xi_1 .$$

The generalised force in the bending mode is only known numerically for $0 \leqslant \xi_1 \leqslant 1{\cdot}0$ as there is no analytical expression for mode shape, but

$$\frac{F_{1g}(t)}{0{\cdot}0406\rho V S a} = 1{\cdot}0 \qquad 1{\cdot}0 \leqslant \xi_1 .$$

Both of these functions are shown in Figs. 1(a) and (b). It should be noted that even though the gust is assumed to be a step, the input functions $L_g(t)$ and $F_{1g}(t)$ are not step functions since the aircraft takes a finite time to penetrate the gust.

3. *Solution of the Equations.*

When the values of ω_1, a, $\hat{t}$, and V appropriate to an aircraft of skin thickness $T = 0{\cdot}375$ in., flying at $M = 2{\cdot}0$ at 40 000 ft are substituted in these equations they become:

$$(D+0{\cdot}525)w-(0{\cdot}0426\,D+5{\cdot}61)z_1 = -\frac{L_g(t)}{\rho VS\hat{t}} \tag{3}$$

and

$$-w+1{\cdot}345\,(D^2+0{\cdot}933\,D+219{\cdot}7)\,z_1 = \frac{F_{1g}(t)}{0{\cdot}0406\rho VSa}. \tag{4}$$

Considering first the stability of the system, the roots of the stability cubic represent a very lightly damped oscillation of 2·36 c.p.s. and $\zeta = 3{\cdot}22$ per cent, together with an aperiodic mode. The coupling of the bending mode with the heaving mode has a negligible effect on the period and damping of the bending mode alone (2·36 c.p.s., $\zeta = 3{\cdot}15$ per cent).

Taking Laplace transforms of the equations and solving for $\bar{z}_1$,

$$\bar{z}_1 = \frac{(p+0{\cdot}525)}{\Delta}\mathscr{L}\left[\frac{F_{1g}(t)}{0{\cdot}0406\rho VSa}\right]-\frac{1}{\Delta}\mathscr{L}\left[\frac{L_g(t)}{\rho VS\hat{t}}\right]$$

where

$$\Delta = (p+0{\cdot}505)\,(p^2+0{\cdot}953\,p+219{\cdot}7)\times 1{\cdot}345.$$

There is a similar expression for $\bar{w}$ but this was not considered further.

Let

$$\bar{z}_1 = \bar{x}_1+\bar{x}_2$$

where

$$\bar{x}_1 = \frac{(p+0{\cdot}525)}{\Delta}\mathscr{L}\left[\frac{F_{1g}(t)}{0{\cdot}0406\rho VSa}\right]$$

and

$$\bar{x}_2 = -\frac{1}{\Delta}\mathscr{L}\left[\frac{L_g(t)}{\rho VS\hat{t}}\right],$$

then

$$z_1(t) = x_1(t)+x_2(t)$$

where $x_1(t)$ and $x_2(t)$ are the inverse transforms of $\bar{x}_1$ and $\bar{x}_2$ and can be considered independently. In each case the expression for the response to a unit impulse function was formulated and the inverse transform was then evaluated using a convolution integral. In the case of $\bar{x}_1$ a simplification was effected by allowing $(p+0{\cdot}525)$ to cancel with $(p+0{\cdot}505)$—a consequence of the small amount of coupling between the modes.

4. *Results.*

4.1. *Response to a Sharp-Edged Gust.*

The solution of the equations of the previous section is shown in Fig. 2(a) and (b). Fig. 2(a) shows

the response z_1 with its component parts x_1 and x_2, the curves having been made non-dimensional by dividing by the steady state value of x_1.

The latter is defined as the steady state solution of the elastic mode in equation (4)

$$1{\cdot}345(D^2+0{\cdot}933\,D+219{\cdot}7)\,z_1 = \frac{F_{1g}(t)}{0{\cdot}0406\,\rho VSa}$$

which gives

$$z_{1_{s.s}} = \frac{1}{1{\cdot}345\times 219{\cdot}7}\,\frac{F_{1g}}{0{\cdot}0406\rho VSa}$$

or, in general form from equation (2)

$$z_{1_{s.s}} = \frac{1}{1{\cdot}414\left(\frac{\hat{t}}{a}\right)\left(\omega_1^2+4{\cdot}415\,\frac{V}{l}\,\frac{a}{\hat{t}}\right)}\cdot\frac{F_{1g}}{0{\cdot}0406\rho VSa}.$$

The above steady state solution represents the deflection of an elastic beam without the alleviating response in heaving, in other words the response of a beam fixed at the nodal points of the mode considered. The steady state solution is a static deflection in a particular mode and allows us to separate the dynamic loading problem into the dynamic and static parts. The actual dynamic loading can be estimated with greater accuracy if the steady state (static part) is computed from static considerations. The dynamic loading is then computed by multiplying the static loading by the non-dimensional dynamic response function as used in this report.

x_2 represents the alleviation due to the aircraft heaving. As t tends to infinity, $x_1(t)$ tends to unity but the complete response $z_1(t)$ tends to zero. We are mainly concerned with possible maximum amplitudes of z_1 and are therefore most interested in the first peak. Since in the present case x_2 is small initially, because of the longer response time of the rigid body mode relative to the bending mode, we can concentrate on x_1 in the first instance.

Within the indicated assumptions, x_1 is the response of a very lightly damped second order system and hence would be expected to have a maximum response to a step forcing function, of approximately twice the steady state value. In Fig. 2(a) it may be seen that the peak value is 1·63 which is appreciably less than 2·0. This is so because, as already pointed out, the forcing function due to a step gust, $F_{1g}(t)$, is not a step function but may be regarded as an 'oscillatory' function followed by a step function. In Fig. 2(b) the x_1 response has itself been broken down into two parts, namely, response to the 'oscillatory' part of the input and response to the step. Both of these responses are oscillatory and of the same frequency but they are out of phase and consequently the peak value of x_1 is less than that due to a step input alone.

The possibility exists that at different conditions of speed and/or aircraft stiffness, these contributions to x_1 will not be out of phase but will, on the contrary, reinforce each other. In order to investigate this, with the minimum of computation time, we considered the effect of altering the time scale of the forcing functions whilst leaving the equations of motion unaltered. It is convenient at this stage to introduce the parameter 'period ratio', defined as the ratio of the time duration of the 'oscillatory' part of the input to the period of the bending mode including aerodynamic stiffness. An increase in period ratio can be regarded in some ways as a decrease in speed since it is an indication of the time taken to penetrate the gust, but to change speed whilst leaving the equations unaltered implies two further assumptions, namely, that $a/\hat{t}$ is kept constant and that the effect of the two terms involving speed explicitly is small (equations (1) and (2)). The assumption of constant $a/\hat{t}$ is equivalent to saying that the heaving response contribution to the bending response is unaltered with changing speed. Keeping constant the terms involving speed explicitly (equations (1) and (2)) implies that changes in speed do not affect the damping

and frequency of the bending mode. It was expected that the effect of the above assumptions on the bending mode response would be small when compared with the effect of changing 'period ratio'. It is shown later by some more rigorous calculations that this simplified calculation gives a very good approximation (e.g. Fig. 4), indicating that the 'period ratio' is the most important parameter. Calculations have been made for various period ratios up to 1·82 and the x_1 responses plotted (Fig. 3). As anticipated, conditions occur where the two parts do reinforce and, for period ratios around 1·3, give peak amplitudes approaching three times the steady state response of x_1. Thus we have the significant result, that, regarding the aircraft as being fixed at its nodal points (i.e. neglecting x_2) the response to a unit step gust can in certain conditions have a peak amplitude approaching three times the steady state value.

These peak amplitudes are shown in Fig. 4 plotted against period ratio. The 'equivalent' Mach number scale is included for an assumed constant height of 40 000 ft. This curve is useful in that it indicates a trend. However, since the assumptions of constant $a/\hat{t}$ tends to over-estimate the damping of the bending mode at lower speeds, certain calculations have been repeated using more appropriate values of the parameters. The following cases have been considered.

M	h	$a/\hat{t}$	$\zeta\%$
0·90	20 000	1·095	3·16
0·42	10 000	0·737	2·42
0·30	S.L.	0·738	2·42

A constant value of 2·0 was assumed for lift slope a.

The results are shown in Fig. 5 and the peak amplitudes included in Fig. 4. Fig. 5 shows that the responses are of the same form as before; Fig. 4 shows that provided the maximum responses are plotted against period ratio (and not Mach number) the curve based on the $M = 2{\cdot}00$ equations provides a very reasonable indication of the variation of the maximum response with speed.

4.2. *Response to a Ramp-Type Gust.*

It has been seen how, due to dynamic overshoot, maximum bending amplitudes of up to three times the steady state values can arise from a sharp-edged gust. The sharp-edged gust is, of course, a mathematical idealisation and the response to gusts having ramps of various lengths, H, is of more practical interest. The ramp-type gust is also an idealisation and in any detailed study the gust inputs should be represented by spectra; however, the ramp could have some physical significance in regions of severe up-draught as, for example, near cumulo-nimbus clouds.

The response to a ramp is immediately obtained again by using a convolution integral but in this case on the total response z_1 to a sharp-edged gust. Since the ramp is bound to reduce the amplitude of the peak response, the most interesting case to consider is that giving a maximum response of nearly 3 to a sharp-edged gust. This has been taken as $M = 0{\cdot}42$, $h = 10\,000$ ft, period ratio 1·1, the response curve being that shown in Fig. 5. The results of the calculations are shown in Fig. 6 where the responses $z_1(t)$ are given for various ramp lengths H. It can be seen that increasing ramp length rapidly reduces the magnitude of the response but it will be noted that with a ramp length of 104 ft, near to the present standard of 100 ft, the peak response is still greater than 2·0. However, the standard of 100 ft is of uncertain significance. It has not been established by observation as a realistic parameter describing gusts but has, nevertheless, for many years enabled a comparison to be made between new aircraft and existing proven aircraft. In this sense it has been useful since aircraft shapes have not altered radically. However, in the case of the slender delta aircraft it is not possible to draw definite conclusions as to the order of bending deflection to be expected on the basis of a 100 ft ramp length. In the present example (Fig. 7, $M = 0{\cdot}42$) for a ramp length of 100 ft, the dynamic overshoot factor is 2·1; for $H = 150$ ft it is 1·2 and for $H = 200$ ft it is 0·9, and there is no positive evidence to indicate which of the ramp lengths should be used. It appears that the only sensible method is to define the gust input by a spectral representation.

It is interesting to compare the effect of ramp length of input on peak response of the slender aircraft considered in this report with that of a simple mass, spring, damper system. The response of a simple mass, spring, damper system, when expressed in non-dimensional form of an overshoot factor, is very similar to the elastic response of an unswept wing to a gust front parallel to wing span. This has been done in Fig. 7 where the abscissa is the product of ω, the frequency of the oscillation, and T the ramp length in time (or the equivalent H in feet divided by aircraft speed). The curve for the simple second order system with zero damping is given by

$$R(T) = 1 + \left| \frac{\sin \omega T/2}{\omega T/2} \right|.$$

It starts at 2·0 and goes to unity at a series of cusps at intervals of ωT of 2π. The effect of a small amount of damping is merely to reduce the peaks and increase the troughs but in all cases the response is greater than or equal to unity. In the case considered, of the aircraft with longitudinal bending, flying at $M = 0{\cdot}42$, the response starts at 2·9 and decreases much more rapidly but this also has minima at ωT values which are near multiples of 2π. These minima are less than unity mainly because of the manner in which the curves are non-dimensionalised; the total response Z, takes into account the alleviating effect due to heave, whereas the steady state value chosen for non-dimensionalising does not. It is in fact the influence of the second degree of freedom on the motion.

In order to estimate the effect of period ratio, the responses were also evaluated for the following case:— $M = 0{\cdot}9$, $h = 20\,000$ ft, period ratio = 0·55. The peak responses are plotted in Fig. 7. The results show no unusual feature, the peak response decreasing steadily in value with increase in ωT and having a value always less than the response of a second order system.

5. *Discussion.*

The longitudinal bending response of a slender delta aircraft to single gust inputs has been considered and the following main conclusions drawn.

Firstly, due to the finite time for immersion of the aircraft into a sharp-edged gust, the dynamic overshoot factor (the maximum non-dimensional value of bending response) is a function of immersion rate and thus of forward speed, in the present report measured by 'period ratio'. In contrast, the dynamic overshoot factor of an unswept wing is independent of immersion rate into a sharp-edged gust, and depends only on the damping ratio of the wing mode considered. For small damping, (say < 8 per cent) the dynamic overshoot factor of a straight wing due to a sharp-edged gust is approximately $(2 - \pi\zeta)$, and thus is always less than 2. For the aircraft considered in this report, where the longitudinal bending is a predominant feature, the dynamic overshoot factor due to a sharp-edged gust is a function of immersion rate (Fig. 4) and its value ranges approximately from 1·5 to 3·0.

The values of dynamic overshoot factors discussed above are decreased somewhat by the aircraft response in rigid modes. In the cases considered in the present report this alleviation, due to heaving only, is of the order of 5 per cent.

Secondly, the bending responses of a slender delta aircraft to ramp-type gusts are similar in character to those of straight wing aircraft, when the dynamic overshoot factor is plotted against the ramp length, Fig. 7; the numerical values, however, can be widely different. Taking as an example the conventional gust of 100 ft ramp length, it is found that the value of the dynamic overshoot factor is 2·1 at a forward speed of $M = 0{\cdot}42$, and 1·45 at $M = 0{\cdot}9$. It is expected that the value of this factor at $M = 2$ would be of the order of 1·5 for a 100 ft long gust.

For the aircraft considered, the maximum value of the dynamic overshoot factor occurs at low speeds; the value of this factor at high speeds appears to be of the same order as for the conventional aircraft. It might be suggested that the problem of gust load magnification due to the longitudinal bending is not so severe as might have been expected. Nevertheless the fact remains, that the values of the dynamic overshoot factor can be much higher for this type of aircraft, when compared with a more conventional design.

The fundamental question is: for what type of discrete gust should this aircraft be stressed? If a typical ramp length of a strong up-draught is less than, say, 100 ft, then the slender delta aircraft can be much worse off than a more conventional layout. If on the other hand, the typical ramp length of an up-draught is of the order of a few hundred feet, then the slender delta aircraft appears to have some advantage over the conventional design.

It might be added that the neglected degree of freedom, pitching, should have a very small effect on the loads due to a short gradient gust. The period of short period oscillations is of the order of 3–4 sec for the type of aircraft considered, i.e., the wavelength of short period oscillations is of the order of 6000 ft to 8000 ft. The response of an aircraft to gusts a few hundred feet long is not strongly modified by a mode of having a wavelength measured in thousands of feet.

More rational assessment of gust loads on a slender delta aircraft can be obtained using power spectral techniques[1, 2]. This is necessary in any case, in order to study the aircraft responses to continuous turbulence. There is evidence that this type of turbulence persists to the highest altitudes flown at present.

6. *Conclusions.*

The values of the dynamic overshoot factor due to the lengthwise bending of a slender delta aircraft can vary within much wider limits than the dynamic overshoot factor due to spanwise bending of a conventional aircraft.

Flying at low speed ($M \simeq 0{\cdot}4$) into a sharp-edged gust produces a value of the dynamic overshoot factor approaching 3.

At higher speeds ($M > 0{\cdot}9$) and for gust ramp lengths greater than 100 ft, the dynamic overshoot factor appears to be less than for a conventional aircraft.

LIST OF SYMBOLS

a	Lift curve slope
D	d/dt
$F(x, t)$	Forcing function
F_i	$\int_0^l F\, w_i\, dx$, generalised force in i^{th} mode
$F_{1g}(t)$	Generalised force in first bending mode due to 1 f.p.s. vertical gust
g	Acceleration due to gravity
h	Aircraft height, feet
H	Gust ramp length, feet
l	Aircraft length in feet
$L_g(t)$	Lift due to 1 f.p.s. vertical gust
$\mathscr{L}$ [function]	Laplace transform
M	Mach number
M_i	Generalised mass in i^{th} mode
p	Laplace transform variable
$R(T)$	Maximum response function of second order system
S	Wing area, ft^2
t	Time, secs
$\hat{t}$	$\frac{W}{g\rho VS}$, units of aerodynamic time, secs
T	Skin thickness, inches
T_1	Length of ramp-type forcing functions, secs
V	Aircraft true speed, ft sec^{-1}
w	Aircraft vertical velocity, ft sec^{-1}
$w_1(\xi)$ or $w_1(x)$	Shape of i^{th} normal mode
W	Total aircraft weight including engines, lb
$x_1(t)$, $x_2(t)$	Bending response functions
x, y	Rectangular co-ordinates, origin at wing apex x axis along aircraft centre-line

LIST OF SYMBOLS—*cont.*

$Z(x, t)$	Solution of beam deflection equation
$z_i(t)$	Response function in i^{th} mode
$z_1(t)$	$x_1(t)+x_2(t)$, total response function in first bending mode
$z_{1_{s.s}}$	Steady state value of z_1
$Z_i(x, t)$	$z_i(t)\, w_i(x)$
ξ	x/l } Non-dimensional co-ordinates
η	y/l }
ξ_1	$V\, t/l$, gust penetration parameter
ρ	Air density, slug ft^{-3}
ζ	Damping ratio of 1st bending mode
ω_i	Natural frequency of i^{th} mode
ω_1	$(480\ T)^{\frac{1}{2}}$, natural frequency of 1st bending mode, sec^{-1}

REFERENCES PART IV

No.	*Author(s)*	*Title, etc.*
1	J. K. Zbrozek	Vertical accelerations due to structural vibrations of a slender aircraft flying in continuous turbulence. A.R.C. C.P. 842. July, 1963.
2	E. Huntley	The longitudinal response of a flexible slender aircraft to random turbulence. A.R.C. R. & M. 3454. August, 1964.

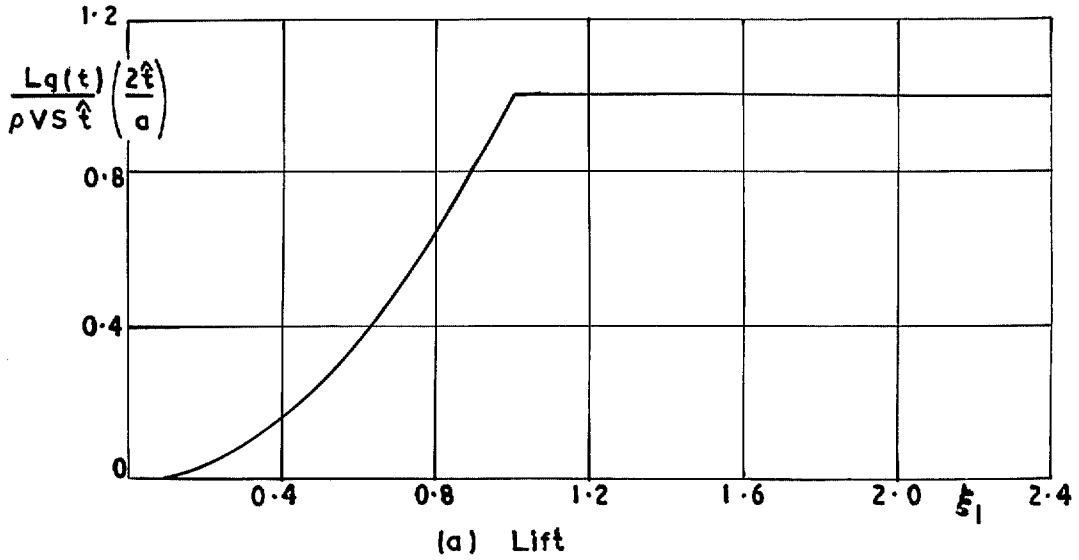

(a) Lift

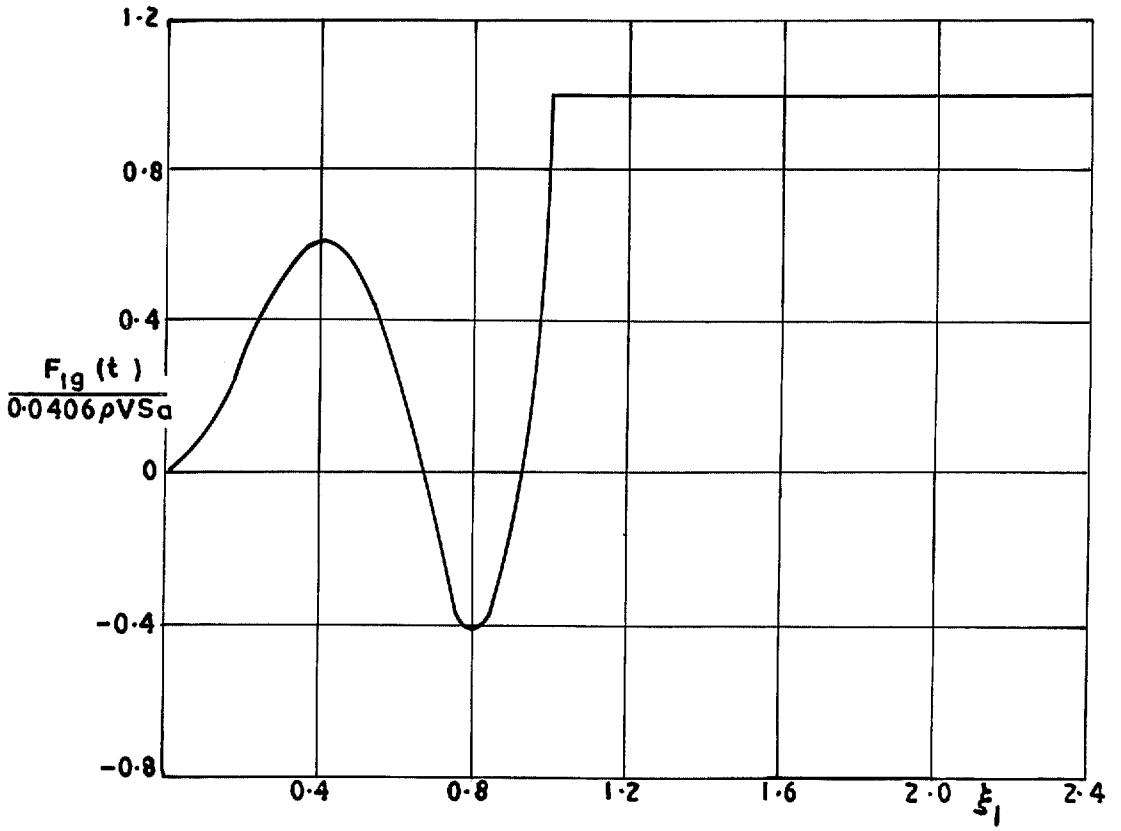

(b) Generalised force in bending mode

FIG. 1. Variation of forcing functions with time.

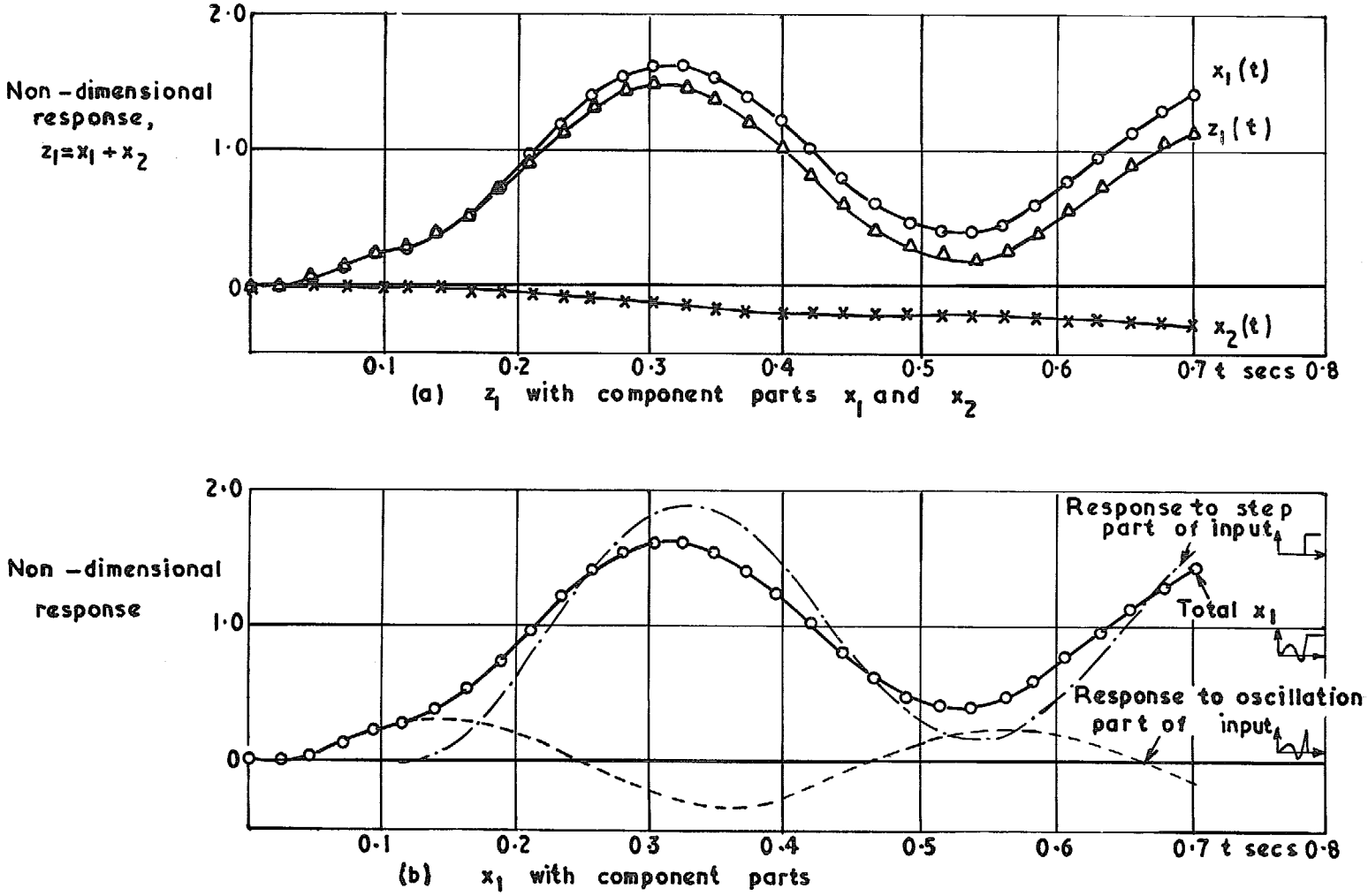

FIG. 2. Deflection in bending mode due to sharp edged gust for $M = 2{\cdot}00$, $h = 40{,}000$ ft.

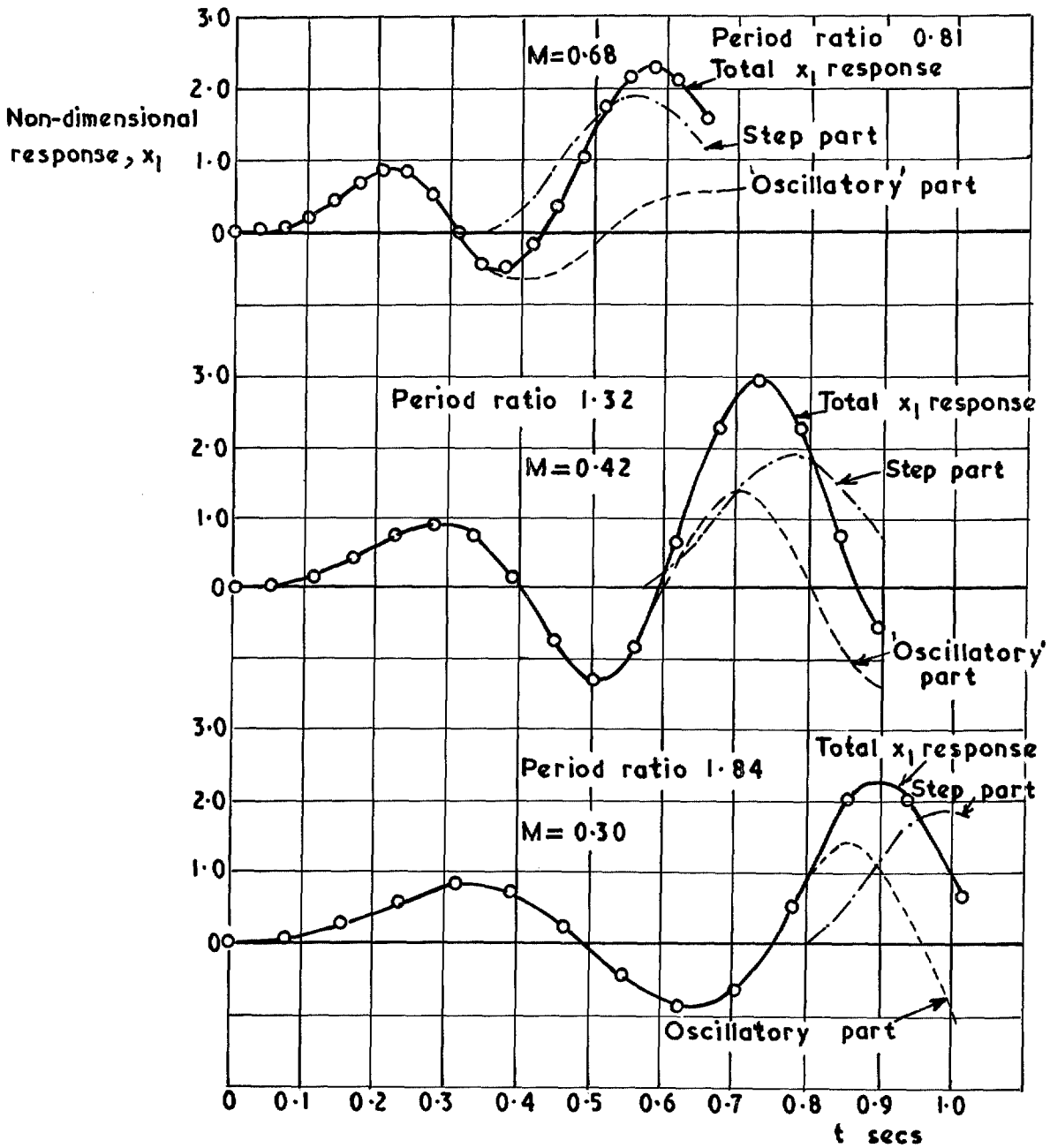

FIG. 3. Components of response to sharp-edged gust. ($M=2{\cdot}00$ equations).

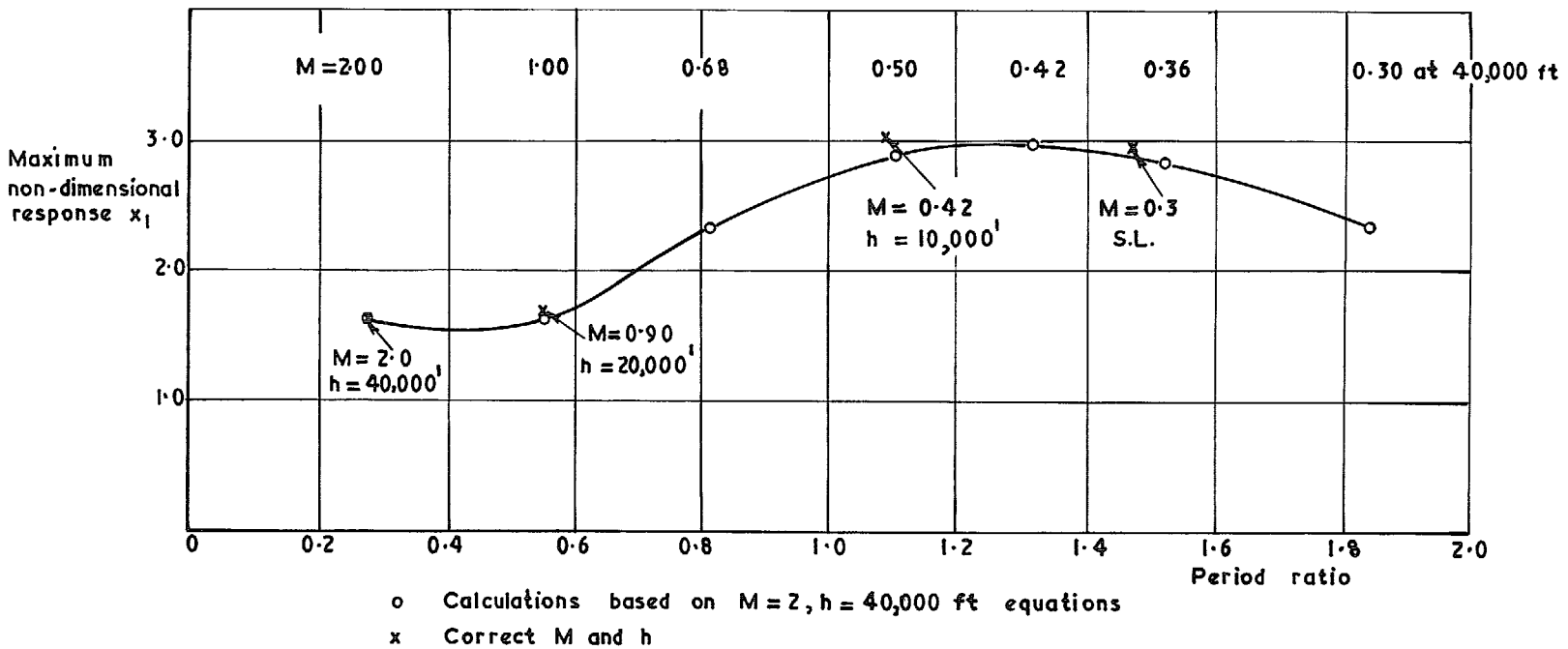

FIG. 4. Response to sharp-edged gust. Variation of maximum deflection in bending mode (with period ratio).

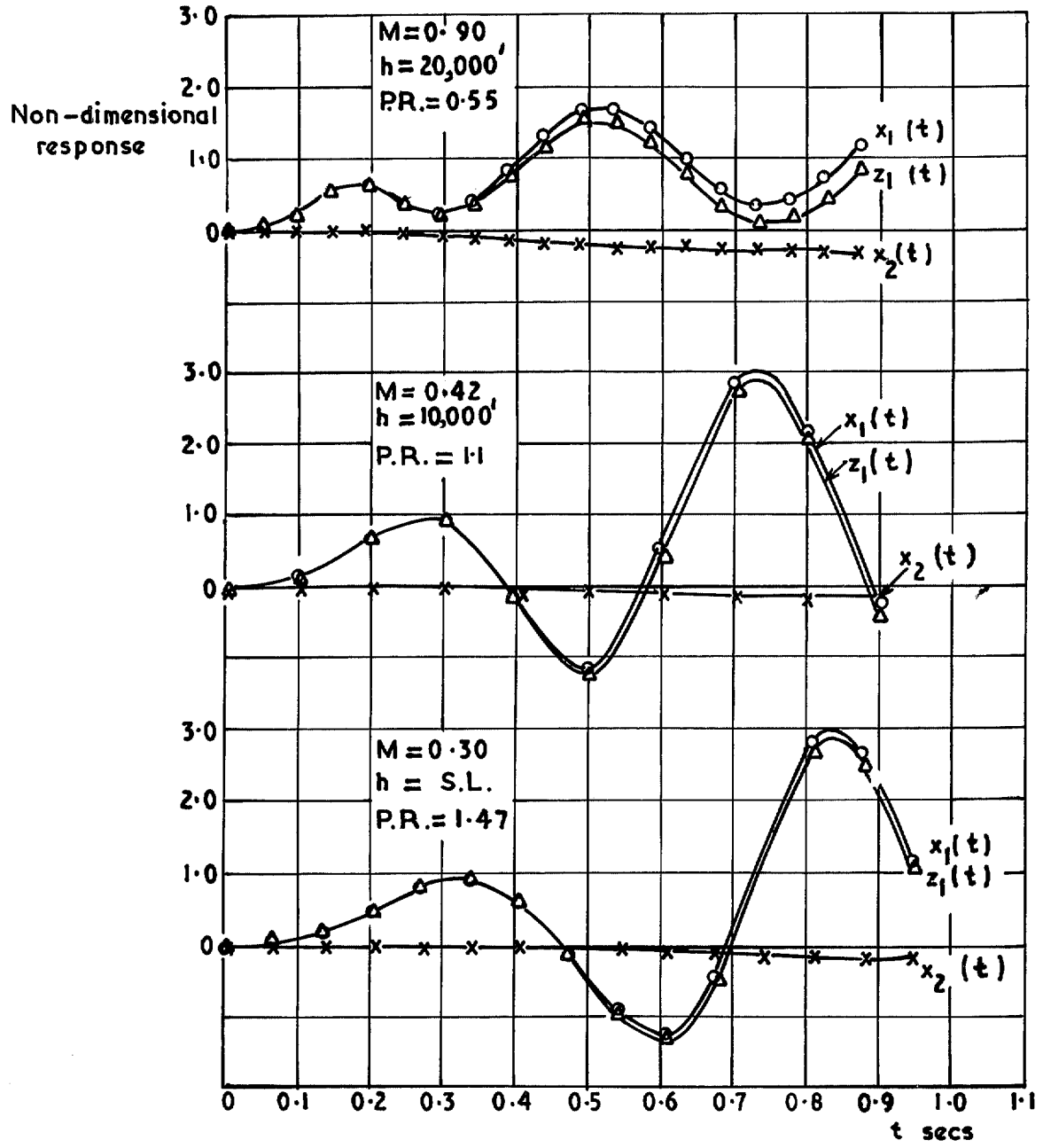

FIG. 5. Response to sharp-edged gust, correct parameters, $M = 0{\cdot}90$, $0{\cdot}42$ and $0{\cdot}30$.

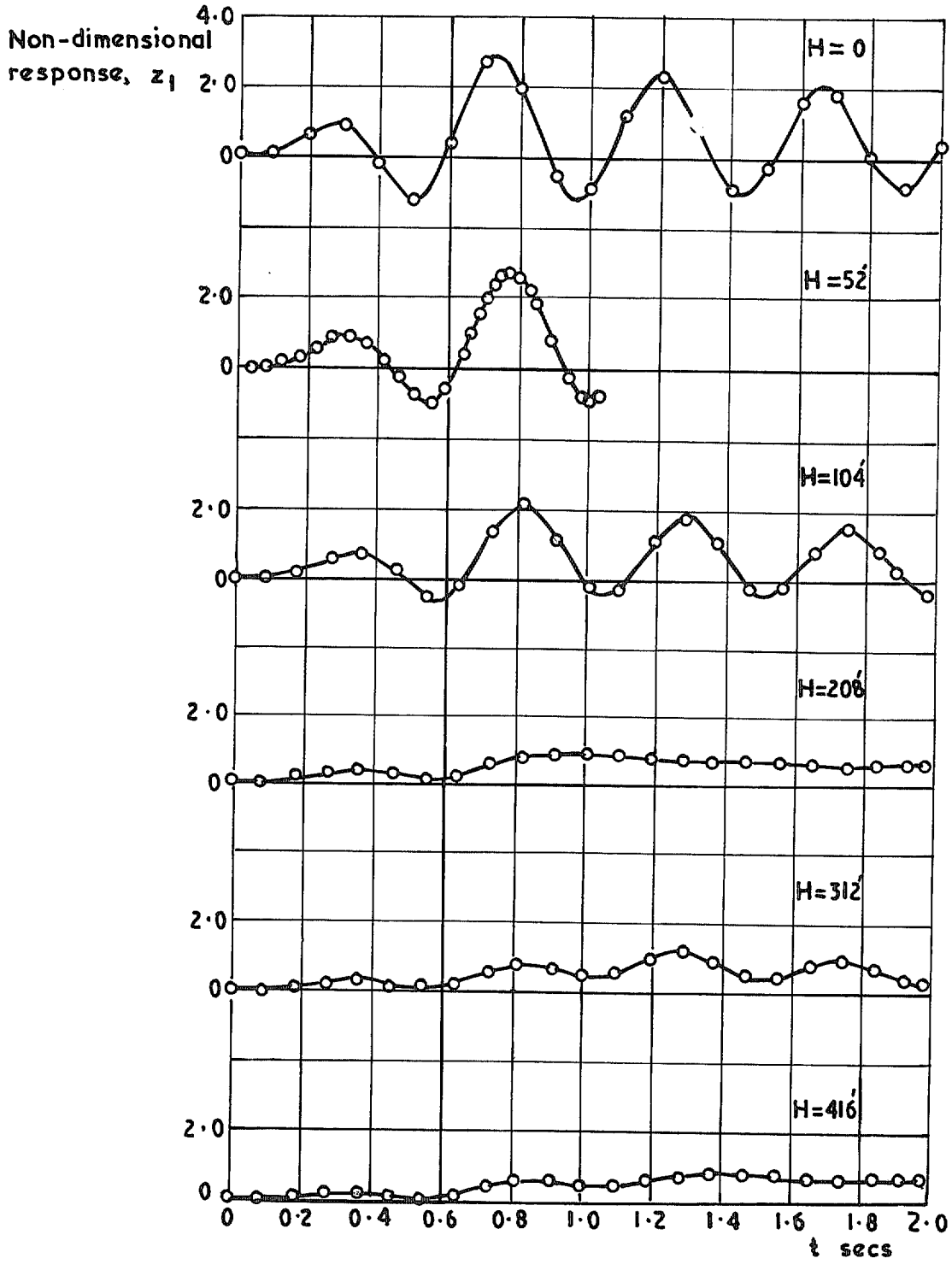

FIG. 6. Effect of ramp length on response to ramp-type gust, $M = 0{\cdot}42$, period ratio 1·1.

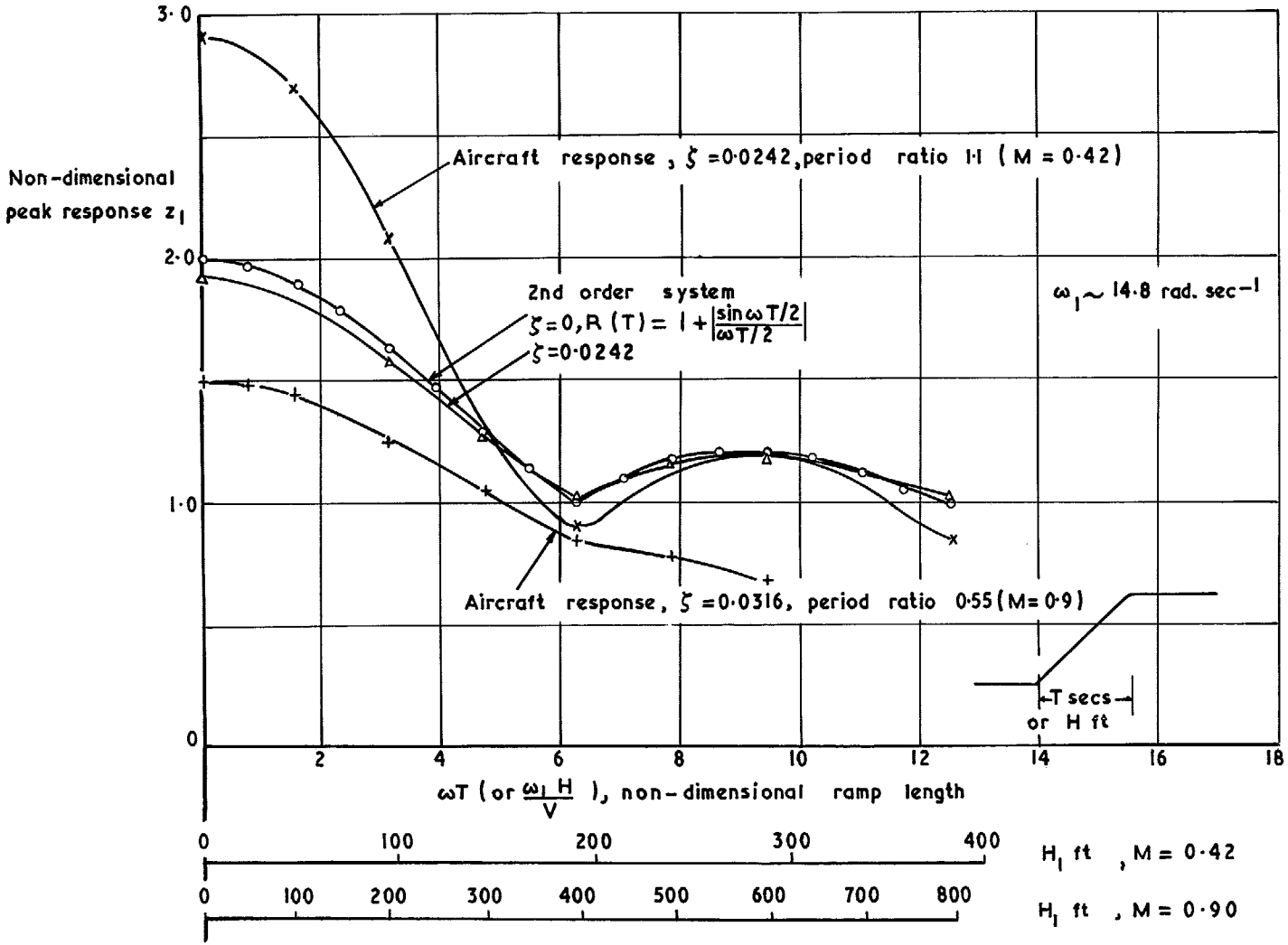

FIG 7. Variation of peak response with ramp length

Printed in Wales for Her Majesty's Stationery Office by Allens Printers (Wales) Limited
Dd. 502110 K.5. 4/72.

HER MAJESTY'S STATIONERY OFFICE

Government Bookshops

49 High Holborn, London WC1V 6HB
13a Castle Street, Edinburgh EH2 3AR
109 St Mary Street, Cardiff CF1 1JW
Brazennose Street, Manchester M60 8AS
50 Fairfax Street, Bristol BS1 3DE
258 Broad Street, Birmingham B1 2HE
80 Chichester Street, Belfast BT1 4JY
Government publications are also available through booksellers

SBN 11 470490 2